Lawrence Berkeley National Laboratory
Recent Work

Title
STRUCTURE AND MECHANICAL PROPERTIES OF Fe-Ni-Co-C STEELS.

Permalink
https://escholarship.org/uc/item/85m4h506

Author
Das, Santosh Kumar.

Publication Date
1968-12-01

eScholarship.org Powered by the California Digital Library
University of California

UCRL-18652

cy. 2

STRUCTURE AND MECHANICAL PROPERTIES OF Fe-Ni-Co-C STEELS

Santosh Kumar Das
(M.S. Thesis)

December 1968

TWO-WEEK LOAN COPY

This is a Library Circulating Copy which may be borrowed for two weeks. For a personal retention copy, call Tech. Info. Division, Ext. 5545

LAWRENCE RADIATION LABORATORY
UNIVERSITY of CALIFORNIA BERKELEY

cy. 2

UCRL-18652

DISCLAIMER

This document was prepared as an account of work sponsored by the United States Government. While this document is believed to contain correct information, neither the United States Government nor any agency thereof, nor the Regents of the University of California, nor any of their employees, makes any warranty, express or implied, or assumes any legal responsibility for the accuracy, completeness, or usefulness of any information, apparatus, product, or process disclosed, or represents that its use would not infringe privately owned rights. Reference herein to any specific commercial product, process, or service by its trade name, trademark, manufacturer, or otherwise, does not necessarily constitute or imply its endorsement, recommendation, or favoring by the United States Government or any agency thereof, or the Regents of the University of California. The views and opinions of authors expressed herein do not necessarily state or reflect those of the United States Government or any agency thereof or the Regents of the University of California.

UCRL-18652

UNIVERSITY OF CALIFORNIA

Lawrence Radiation Laboratory
Berkeley, California

AEC Contract No. W-7405-eng-48

STRUCTURE AND MECHANICAL PROPERTIES OF Fe-Ni-Co-C STEELS

Santosh Kumar Das

(M.S. Thesis)

December 1968

TABLE OF CONTENTS

ABSTRACT

I. INTRODUCTION..... 1

II. EXPERIMENTAL PROCEDURE..... 3

A. Heat Treatment and Mechanical Tests..... 3

B. Electron Microscopy and Fractography..... 4

III. RESULTS..... 5

A. Mechanical Properties of Tempered Martensite and Bainite..... 5

B. Structure of Martensites..... 9

C. Structure of Tempered Martensite.....13

D. Structure of Bainite.....15

E. Electron Fractographic Observations.....18

IV. DISCUSSION.....19

A. Morphology of Martensite.....19

B. Morphology of Bainite.....23

C. Toughness of Tempered Martensite and Bainite.....24

D. Design of Alloys.....29

V. CONCLUSIONS.....31

ACKNOWLEDGEMENTS.....33

REFERENCES.....34

TABLES.....37

FIGURE CAPTIONS.....41

FIGURES.....46

STRUCTURE AND MECHANICAL PROPERTIES OF Fe-Ni-Co-C STEELS

Santosh Kumar Das

Inorganic Materials Research Division, Lawrence Radiation Laboratory,
Department of Materials Science and Engineering of the
College of Engineering,
University of California, Berkeley, California

ABSTRACT

The structure and mechanical properties of tempered martensite and bainite were investigated in a series of steels with varying C, Ni and Co contents. At similar M_s temperatures, the martensite in the 0.24% carbon steels exhibited very small amounts of twinning compared to the 0.4% carbon steels. At equivalent yield and ultimate tensile strength levels the mainly untwinned martensite showed considerably higher toughness than the heavily twinned ones. The addition of cobalt promoted autotempering of martensite by raising the M_s temperature. But its addition in excess of 4% had a deleterious effect on toughness.

The structure of lower bainite showed laths or plates of ferrite with internal carbides but no internal twins. The strength and toughness of isothermally transformed lower bainite was found to decrease with increasing transformation temperature. This was associated with increased coarsening and grain boundary precipitation of the carbides at higher transformation temperatures. At similar strength levels the toughness of lower bainite was found to be superior to the heavily twinned martensite, but inferior to that of the mainly untwinned martensite. Thus, the role of microtwins in lowering the toughness has been demonstrated in two ways. Firstly by comparison between the heavily twinned and mainly untwinned martensite and secondly by comparing the martensite with bainite.

I. INTRODUCTION

In recent years considerable interest has grown in the properties of bainitic structures in steels. High strength bainitic steels obtained both by isothermal transformation[1] and continuous cooling,[2,3] have been successfully developed. Nevertheless, considerable doubt exists as to whether at equivalent strength levels the bainitic structure is tougher than the tempered martensitic or not. Davenport et al.[4] have shown that in a plain carbon steel (0.74% C) the toughness of bainite obtained by isothermal transformation at 580°F is higher than that of tempered martensite. They attributed this brittleness in quenched and tempered steels to the presence of micro-cracks. Similar advantages of bainitic structures have been reported by Waterhouse.[5] The work on 9Ni-4Co-0.45C high strength steel has also established the superior toughness of bainite over tempered martensite at equivalent strength levels.[1] Klinger et al.[6] and also Hehemann et al.[7] in their investigations of AISI 4340 and other steels found the isothermally transformed bainitic structure to possess better toughness than tempered martensitic structures. On the other hand, opposite results have been reported by others.[8-10] These latter workers found the toughness of bainitic structures to be poorer than the conventional quenched and tempered ones. It is interesting to note that they had either low carbon (~0.2% C) steels[8] or their isothermal transformation temperatures were too high (above 700°F).[9,10] Very little data are available for comparing tempered martensite with continuously cooled bainite, which are of great commercial value. To obtain a fully bainitic structure by continuous cooling, a high bainitic hardenability is essential to avoid other transformation products. Even then are are chances of some austenite transforming to

martensite, which severely impair the toughness. However, the present work is limited to only isothermally transformed bainites.

From the previous work, as described above, it seems that probably in certain cases tempered martensite may possess better toughness than bainite of similar strength levels, and in certain cases it may not. In the present work an attempt has been made to investigate whether such variations exist or not and if so why? Transmission electron microscopy has been used to determine the structural differences that may lead to such variations in notch toughness in steels.

There have been suggestions[11,12] that the presence of internal twins in martensite may reduce its ductility. So one of the aims of the present work was to see whether micro-twins have any influence on notch-toughness or not. It has also been argued that the extent of internal twinning in martensite may partially depend on martensite start (M_s) temperature of steels, and the lower the M_s temperature, the greater is the tendency for martensite to twin rather than to slip. Since carbon and nickel are known to lower M_s temperatures and cobalt to raise it, alloys at two different carbon levels, 0.24% and 0.4%, were chosen with varying nickel and cobalt contents. Thus by adjusting nickel and cobalt contents it was possible to have the same M_s temperature in steels of different carbon levels. This was necessary to assess the role of individual alloying elements on the occurrence of internal twinning in martensite apart from their influence on M_s temperature. The composition of the alloys designed on the above basis are given in Table I along with their M_s temperatures. The steels will be referred to by their heat numbers as given in Table I.

II. EXPERIMENTAL PROCEDURE

A. Heat Treatment and Mechanical Tests

The specimens were austenitized at 1600°F for one hour in an argon atmosphere and then either water (for 0.24% C steels) or oil quenched (for 0.4% C steels). Then they were immediately refrigerated in liquid nitrogen for 10 hours to ensure complete transformation to martensite. The tempering was done in a neutral salt bath. All the specimens were double tempered for 4 hours at different temperatures, i.e. tempered for 2 hours, water quenched, then refrigerated, and finally tempered for another 2 hours. This completely eliminates the retained austenite. To obtain the bainitic structures the specimens were directly quenched into the salt bath at required temperature and then isothermally transformed. The heat given out by the specimen was very small compared to the volume of the salt bath and so there was no appreciable rise in the temperature of the bath. After heat treatment all the specimens were carefully ground from both sides using excessive coolant, to remove the decarburized layer, if any. The carbon analysis before and after the heat treatment showed no significant decarburization.

The tensile specimens whose dimensions are shown in Fig. 1 (a) were 0.060 in. thick. Fatigue precracked Single Edge Notch (SEN) specimens Fig. 1 (b) were used for measuring notch toughness. All the specimens were precracked in tension-tension fatigue. These were tested at -196°C to obtain plane-strain conditions in these 0.060 in. thick specimens. Even then plane-strain conditions were not obtained in some cases. These non-standard SEN specimens are economical, especially when large number of tests have to be made in order to obtain some indication of notch toughness.

All the tensile and notch toughness tests were done on an Instron machine at a cross head speed of 0.1 cms/min. The room temperature notch toughness values were obtained on half-inch thick specimens shown in Fig 1 (c). These specimens were fatigue pre-cracked and tested on MTS.

B. Electron Microscopy and Fractography

The heat treated 0.060 in. thick specimens were first mechanically ground and then chemically thinned in a solution of 1:1 phosphoric acid and hydrogen peroxide (30%) to about 5 mils. These were electropolished first in perchloric-acetic acid (1:10) solution which gave a rapid thinning. The final electropolishing was done in chromic-acetic acid solution (75 gms CrO_3 + 400 ml acetic acid + 20 ml H_2O) at 25 volts and at a temperature of 20°C. Thin foils were examined in a Siemens Elmiskop I microscope, operated at 100 KV.

The fracture surface of notch specimens were replicated with cellulose-acetate tape. It was shadowed with platinum-palladium (80:20) at a 45° angle and then carbon was evaporated onto it. The tape was subsequently dissolved in acetone and the carbon replica was examined in the electron microscope operated at 60KV.

III. RESULTS

A. Mechanical Properties of Tempered Martensite and Bainite

The mechanical properties of tempered martensitic structures are tabulated in Table II and those of bainitic structures in Table III. It is important to compare the toughness of various structures at the same yield and ultimate tensile strength levels. So each steel was tempered at various tempering temperatures for the same time. This gave a range of strength levels, so that the toughness could be compared at any desired strength level.

The variation of strength and toughness with tempering temperatures are plotted in Fig. 2 through Fig. 7. The high carbon steels 522, 523, 524, (Figs. 2, 3 and 4) show similar tempering characteristics. As expected the yield and ultimate tensile strengths drop and elongation increases with increasing tempering temperature. But the notch toughness shows an embrittlement when tempered around 800°F. Pascover and Matas [1] observed an embrittlement around 900°F in a steel with composition similar to that of 522 but with higher silicon content. The lower silicon alloy did not show any appreciable embrittlement in the room temperature tests. But the present results show that under severe testing conditions at liquid nitrogen temperatures small amount of embrittlement can be seen even in the lower silicon alloys. At the same tempering temperatures the strengths of steels 522 and 523 are nearly the same but those of 524 are always higher. The steel 523 has higher nickel and 524 has higher cobalt than 522. It seems that nickel does not increase the tempering resistance of martensite much, but cobalt has got a great influence in increasing the tempering resistance.

Figures 5, 6, and 7 show the tempering behavior of steels 141, 142, and 145 respectively. Here again the ultimate tensile strength decreases with increasing tempering temperature but the yield strength remains more or less constant in the temperature range shown. The elongation increases continuously but the notch toughness first decreases up to 800°F and then increases on increasing the tempering temperature. This behavior is different from those obtained by Pascover and Matas[15] in CVN room temperature impact tests of a steel similar to 141. Their results show a small increase in the toughness up to 800°F after which it rises sharply. So in this case also there is an appreciable embrittlement around 800°F when the notch toughness tests are carried out at -196°C.

The notch toughness values obtained at various yield and ultimate tensile strength levels are shown in Figs. 8 and 9 respectively. The notch toughness values in the embrittled condition are poor and have not been included in these. There is a bit of scatter in the toughness values obtained for 0.24% carbon steels. However, they are within the band shown. Because of the low A_s temperatures the maximum tempering temperature was restricted to below 1100°F except for steel 524 and so the yield strengths of 0.4% carbon steels could not be brought to exactly the same level as the 0.24% carbon steels. However, it is seen that at similar yield and ultimate tensile strength levels the toughness of the steels 141, 142 and 145 are higher than those of 522, 523 and 524. It is to be seen that the toughness of steel 524 is lower than that of 522. They have nearly the same composition except that steel 524 has 4% cobalt. So also, the steel 145 has lower toughness values than 142, the former having 7% cobalt and the latter 4% cobalt, other alloying elements remaining same. But increasing cobalt from zero to 4% between steels 143 and 140 does not cause an

appreciable decrease in toughness. This shows that other factors remaining same, the increase in cobalt content beyond 4% or so reduces toughness at the same strength level. This embrittling effect of cobalt being more pronounced at higher carbon level.

Steels 140 and 143 with low nickel (5%) contents showed much lower notch toughness compared to the steels 141, 142 and 145 (Table II). This is because the transition temperature of these low nickel steels are much above the test temperature, (-196°C). On the other hand the transition temperatures of the high nickel steels are very near the test temperature.

The mechanical properties of the bainitic steels are given in Table III. It can be seen that for steels 522 and 524, increasing the isothermal transformation temperature results in lower yield and ultimate tensile strengths and also a lowering of the notch toughness. The best properties of bainite are obtained at the lowest possible transformation temperature above M_s. The yield strengths obtained in the as-transformed bainite of steels 141, 143 and 145 are poor compared to the tempered martensites of the same steel. On tempering, the yield strength was found to rise but the ultimate tensile strength decreased slightly. The transmission electron microscopic observations (to be discussed later) showed the presence of martensite in these as-transformed bainite samples. This means that the austenite did not transform completely to bainite even after isothermal holding for 24 hours, and on cooling to room temperature this austenite transformed to martensite. The presence of this virgin martensite gave poor yield strength. On tempering this virgin martensite the yield strength increased. It can be seen that the increase in yield strength was greater for greater amount of martensite present. The steel 143 with 5% nickel had the least amount of martensite and so

the increment was minimum. The steel 145 with 12 Ni - 7 Co had maximum amount of martensite after transforming for 24 hours. This is expected because increasing nickel, increases the incubation period, where as increasing cobalt reduces the incubation period. The notch toughness values also increased on tempering, depending on the amount of martensite present. For the steels 141 and 143 the notch toughness values of tempered bainite are almost same as the transformed bainite within the limits of experimental scatter. Tempering of the bainite in steels 522 and 524 showed no increase in yield strength and toughness, but rather a small drop in strength level, meaning thereby that the transformation to bainite was complete in these two steels. The structural observations also verified this, as will be discussed later.

To compare the notch toughness of bainite and tempered martensite at equal strength levels, the interpolated values for notch toughness of tempered martensite at the same strength level as that of bainite were taken from the curves in Figs 2-7. They have been given in Table IV. It can be seen that the notch toughness of the tempered bainite of steels 141 and 145 are much inferior compared to the tempered martensite. Although 100 percent bainite could not be obtained in these two steels, still it can be seen that as the amount of bainite increased from the steel 145 to 141 the toughness decreased markedly. This clearly shows that at equivalent strength levels the toughness of bainite in these 0.24% carbon steels is inferior to that of tempered martensite. In the steels 522 and 524, the bainitic structures show better notch toughness than tempered martensitic at similar strength levels. This toughness difference is greater at lower isothermal transformation temperature of 500°F for steel 522 than the steel 524, transformed at 550°F.

The superior toughness of the bainitic structure compared to the martensitic is well established[1] for the commerical 9 Ni - 4 Co - 0.45 C steel, which is steel 522 in this work. Also it has been observed[1] that at -196°C the toughness of bainite is not so much greater than that of martensite, but at room temperature the bainite has much higher toughness. In the present case also the toughness of bainite at liquid nitrogen temperature is not so much greater than the tempered martensite in steels 522 and 524. But the room temperature K_{IC} values obtained on half-inch thick specimens showed a large difference.

Summarizing the above results we can say that at similar yield and ultimate tensile strength levels, among the tempered martensitic structures the steels 141, 142 and 145 show better toughness compared to the steels 522, 523, and 524. As will be seen later the structural observations showed the steels 141, 142 and 145 with 0.24% carbon to contain much less twinning compared to the steels 522, 523, and 524 with 0.4% carbon. The notch toughness of the bainite in the steels 141 and 145 are poor compared to the tempered martensite. On the other hand the toughness values of bainite in steels 522 and 524 are better than that of the tempered martensite. Increasing cobalt content of the alloys from 4 to 7 percent reduces their toughness, the effect being greater at higher carbon content.

B. Structure of Martensites:

The structure of martensite of steel 140 is shown in Fig. 10. The structure as seen in Fig. 10(a) has been called needle-like martensite by Kelly and Nutting[12,16] lath martensite by Speich and Warlimont,[17] and massive martensite by Owen et al.[18] Here they will be referred to as

dislocated martensite laths. The selected area diffraction patterns (not shown here) from the areas near A and B show them to be in [111] and [100] orientation respectively. So these parallel laths are separated merely by low angle boundaries. A trace analysis of the long direction of the laths indicated them to be in ⟨111⟩ direction as has been observed before.[12] In some other regions [Fig. 10(b)] multidirectional plates were also observed. Thus the martensite in this steel is a mixed structure of laths and plates. There are also some precipitates of carbide in this freshly quenched martensite, as can be seen in Figs. 10(b) and (c). These platelets of carbide did not give a sufficiently satisfactory diffraction pattern to be identified, but the trace analysis of the habit plane of the precipitates showed them to be {110}. This indirectly proves that the precipitates that are formed in this steel as a result of autotempering are cementite which show {110} habit, in agreement with the results of Page et al.[19] This is different from the results of Banerjee,[20] who found the autotempered precipitates in AISI 4340 steel to be ϵ-carbide.. Probably the autotempered precipitates are ϵ-carbide in high carbon steels but are Fe_3C in low carbon steels. There was very little twinning found in this steel.

The morphology of martensite in steel 142 is similar to that of 140 and is shown in Fig. 11. Figure 11(a) shows martensite laths with no twinning at all. Isolated examples of internal twins were seen in some plates as in Fig. 11(b). This steel also has a mixture of lath and acicular martensite with small amount of twinning. The martensite of steel 143 shows a small amount of twinning (Fig. 12). The twins are rather unevenly distributed as can be seen in Fig. 12(a) and (b). Sometimes twins were restricted to a very small region near the edge of the plate instead

of mid rib as in Fig. 12(c). This kind of morphology has also been observed by Warlimont.[21] Figures 13(a) and (d) show twinning in martensite of steel 145. The dark field of $(0\bar{1}1)$ twin reflection [Fig. 13(c)] lighted up the twins in lath A and also the adjacent lath B. When dark field was taken of the $(0\bar{1}1)$ matrix reflection it reversed contrast for lath A only (not shown here). This shows that the laths A and B are twin related. It is to be noted that these two laths are 0.5 to 1.0μ wide, where as the laths that are merely separated by low angle boundaries are about 0.25μ wide [Figs. 10(a), 11(a), 13(d), etc.]. Figure 13(d) shows a packet of parallel laths of the same orientation formed within an original austenite grain. It was frequently found that a group of such parallel laths were separated by a high angle boundary from another group. An example of this is shown in Fig. 14(a). The selected area diffraction pattern [Fig. 14(b)] of a group of laths shows two bcc orientations as indexed in Fig. 14(b). The dark fields of spots A and B reverse contrast for the laths in [111] and [100] orientations respectively.

An examination of a number of micrographs revealed the amount of lath martensite in steel 143 to be less than in steel 140. This 143 has the same composition as steel 140 but has no cobalt in it. Also between steels 142 and 145 the latter showed comparatively more lath martensite than the former. They also have identical compositions except that steel 145 has higher cobalt than steel 142. These comparisons show that the addition of more cobalt increases the proportion of untwinned lath martensite.

In all the 0.24% carbon steels the structure was predominantly lath martensite with a small amount of internally twinned plates. In most cases twinning was restricted to the mid rib. On the other hand many examples of completely internally twinned martensite plates were found

in the 0.4% carbon steels 522, 523 and 524 (Figs. 15-18). Figures 15(a) shows an extensively twinned martensite plate of steel 522. Some small martensite plates were also found to be completely twinned [Fig. 15(b)]. Very often the fine internal twins gave rise to streaks in the ⟨112⟩ directions in the diffraction patterns as can be seen in Fig. 16. In addition to the twin spots there are other extra spots due to double diffraction [Fig. 16(c)]. The twins are not as clearly resolved in the bright field, as in the dark field of the $(\bar{1}10)$ twin spot, [Fig. 16(b)]. This reflection also reverses the contrast for the adjacent plate showing that they are twin related. A very high density of twins can be seen in the mid rib in Fig. 17. The dark field of the streaks [shown by the position of the objective aperture offer the streak in the inset of Fig. 17(b)] reverses the contrast for twins. The martensite of steel 524 also showed varying amounts of twinning in different regions as seen in Fig. 18.

A quantitative comparison of the volume fraction of twins among the various alloys is rather difficult. Because in most cases it is necessary to tilt the foil to bring the twins in good contrast and also it is essential to take a dark field of the twin reflection to verify whether they are really twins or not. However by examining a number of foils a relative comparison was made. It was found that the volume fraction of the twins in all the three 0.4% carbon steels was much higher than the 0.24% carbon series, irrespective of their M_s temperatures. The steels 142 and 524 have nearly the same M_s temperatures but the extent of internal twinning is much less in 142 compared to 524. This means that although by adjusting substitutional elements like nickel and cobalt, the M_s temperatures of the steels having different carbon contents can be made the same, the extent of internal twinning can still be widely different.

C. Structure of Tempered Martensite

The microstructures of martensite tempered at various temperatures were examined. The martensite of the 0.4% carbon steels tempered at 400°F showed mainly ε-carbide with small amount of Fe_3C which, has also begun to precipitate. Figure 19 shows twinned and untwinned regions of 400°F tempered martensite of steel 522. The twins can be very clearly seen in the dark field micrograph in Fig. 19(b). The fine precipitates of ε-carbide can be seen in between the twins, wherever the twin spacings are large and they do not form on the twin boundaries. In many cases these precipitates do not give a satisfactory diffraction pattern to be identified but the trace analysis of the habit plane shows a $\{100\}_\alpha$ habit. It is known[22,23] that the ε-carbide has $\{100\}_\alpha$ habit and also grows in $\langle 100\rangle_\alpha$ direction. Whenever suitable diffraction patterns were obtained, it was possible to take the dark field of the carbide spot [Fig. 19(d)], which positively identified them to be ε-carbide. In some regions cementite of {110} habit has also begun to form as can be seen clearly at A in the dark field micrograph in Fig. 19(f), in the martensite plate that is in [100] orientation. The dark field was taken from a spot which had reflections from adjacent laths, from Fe_3C and from ε-carbide superimposed on it and so it reversed contrast for all of them. This is because the interplanar spacings of $(100)_\alpha \approx (022)_{Fe_3C} \approx (101)_{\epsilon\text{-carbide}}$.

On increasing the tempering temperature ε-carbide was replaced by Fe_3C. In the presence of twins the cementite precipitated preferentially on the twin boundaries with {112} habit. In the absence of internal twinning the cementite precipitated in Widmanstatten pattern with {110} habit.

Figure 20 shows the structure of martensite of steel 524 tempered at 800°F. At this tempering temperature the precipitates were all found to be cementite. The precipitation of cementite on twin boundaries and on the grain boundaries can be seen in Fig. 20(c). Figure 21 shows the twinning and untwinned regions obtained after tempering at 1100°F in steel 522. The carbides can be seen to be aligned up unidirectionally along the twin boundaries [Fig. 21(a)]. There are also precipitates along the grain boundary. Similar observations have been made by Baker et al.,[24] but they did not observe carbides at the martensite plate boundaries in the presence of twins. Figures 20(c) and 21(a), (b) and (c) clearly show that cementite does precipitate at the grain boundaries even in the presence of twins. Frequently the twins are not very clear due to the presence of carbides but by tilting they can be brought to better contrast as in Fig. 21(c). This shows that it is not easy to remove the twins, unless recrystallization occurs, which will be at higher temperatures than 1100°F. Spherodization of carbides has also begun at this temperature of 1100°F [Fig. 21(d)] in the twin free region. The structure of tempered martensite in steel 523 is also similar to 522. It also shows precipitation at twin boundaries in the presence of twins, Widmanstatten precipitation in the absence of twins and also precipitation of carbides at martensite plate boundaries.

Unlike the high carbon steels, tempering of 0.24% carbon steels at 400°F showed mostly cementite possibly with a small amount of ϵ-carbide. At 600°F it showed almost all cementite. Figures 22(a) and (b) show 400°F and 600°F tempered martensite in steels 141 and 145 respectively, where the carbides are mostly Fe_3C. Since the martensite in these steels show very little twinning, the cementite precipitated predominantly in

the Widmanstatten pattern with {110} habit wherever small amounts of twins were present cementite precipitated preferentially along the twin boundaries. At 600°F the precipitation along the lath boundaries is not observed but on tempering at 1000°F small carbide precipitates can be seen at the lath boundaries as in Fig. 23(a) and (b) and Fig. 24(c) for steels 142 and 143 respectively. But it is to be noted that in all these cases the carbides at the lath boundaries are not continuous all along the boundary. In spite of these small boundary precipitates, the steel 142 showed very high toughness as has been seen before. The fractographic observations also did not show intergrannular failure as will be discussed later.

D. Structure of Bainite

The structure of lower bainite is known[25,26] to consist of acicular ferrite with carbides at 55-65° to the long direction of ferrite. The transition from lower to upper bainite is known to occur in a relatively narrow temperature range around 650°F. As discussed before, the strength and toughness deteriorated with increasing isothermal transformation temperature, even in the lower bainite range. Hence the structure of lower bainite with increasing isothermal transformation temperature were examined. Figures 25, 26 and 27 show the structures of bainite isothermally transformed at 500°F, 550°F and 600°F respectively for steel 522. Although in some regions the classical lower bainite structure is not so obvious [Figs. 25(a) and 26(a)], it can be clearly seen in other regions [Figs. 25(b), 26(b) and 27(a)]. The carbide particles were found to become coarser with increasing isothermal transformation temperature which is consistent with the decrease in strength. Also on isothermal transformation at 600°F the carbides start precipitating

at the plate boundaries as is clearly seen in Fig. 27. The dark field micrograph of the cementite spot reverses the contrast for the carbides which positively shows that the black markings at the boundaries are cementite. The lower bainite formed at 550°F in steel 524 is similar to that of 522 (Fig. 28). In Fig. 28(a) the carbide plates can be seen in an extensive matrix, which is very similar to that of Fig. 25(a). These are ferrite plates with internal carbides rather than laths. Sometimes very long carbides are also seen as in Fig. 28(c). This variation in carbide size is obviously a sectioning effect. By trace analysis the habit plane of these carbides was shown to be {112} habit in all the cases.

At higher transformation temperatures, in the low carbon steels, bainite laths were observed instead of plates. These laths were found to be placed side by side with only a very slight misorientation between them. This is seen very clearly in Figs. 29 and 30, which show the structure of the bainite of steels 141 and 143 isothermally transformed at 620°F and 670°F respectively. The selected area diffraction pattern [Fig. 29(c)] of a group of laths shows a single bcc [111] orientation only with a very slight misorientation. The dark field of $(1\bar{1}0)$ reflection lights up alternate laths only. The dislocations in the other laths are also brought into contrast. This is also seen in Fig. 30 where dark field of $(1\bar{1}0)$ relfection brings out the alternate laths in contrast. Here the laths are nucleated on either side of the prior austenite grain boundary, which is very similar to the structure of martensite in Fig. 10(a) except that there are carbides inside these bainitic ferrite laths. It is also seen that the number of carbide particles are very few in these low carbon bainites, compared to the high carbon ones, which is expected. It is also interesting to note that there is no precipitation at the lath boundaries in the 0.24%

carbon bainite although they were formed above 600°F, while the 0.4% carbon bainite showed lath boundary precipitation. In no case was internal twinning observed in the bainitic ferrite. The precipitation of cementite on the twin boundaries does not remove internal twins in martensite even on tempering above 1000°F as has been seen before [Fig. 21(c), 23(c) and 24(a) and (b)]. Thus, if there were internal twins in the bainitic ferrite laths they could not have been removed by precipitation of cementite on holding for four hours at 550°F [Fig. 26].

As has been mentioned before the bainite reaction in the steels 141, 142, 143 and 145 did not go to completion even after isothermal holding for 24 hours. When examined the structures showed some areas of martensite, which formed from the untransformed austenite on cooling after isothermal transformation. Sometimes it becomes very difficult to distinguish between the martensite and the bainite that contains a few or no internal carbides, because they appear to be very much alike. To verify that they were martensite and not bainite tempering was done again after isothermal transformation. After tempering Widmanstatten precipitates of carbides were observed in the martensitic areas that were formed from untransformed austenite. The steels 141 and 143 showed a small amount of martensite. Even after transforming for 24 hours, only a small amount of bainite was obtained in steel 142 and the steel 523 showed no bainite at all but only martensite. But almost 100 percent bainitic structure was obtained in steels 522 and 524. These can be understood by the effect of the composition on the T-T-T-diagrams.

E. Electron Fractographic Observations

The fracture surface of notched specimens tested at liquid nitrogen temperature were examined for the fracture mode. The tempered martensite of the low carbon steels with very high toughness values showed dimpled rupture. An example of this is shown in Fig. 31 which was taken from steel 142 tempered at 400°F. The dimples are slightly elongated and are typical of transgranular fracture by microvoid coalescence. Figures 32(a), (b) and (c) show the fracture surface of martensite of steel 522 tempered at 400°F, 800°F and 1000°F, respectively. In all cases the fracture appears to be quasi cleavage. There appears to be no intergranular failure. The fracture surface of bainite of steel 522 transformed at 500°F also showed predominantly quasi-cleavage facets with groups of dimples [Fig. 33(a)]. Very near the surface of the specimen elongated dimples in the small shear lip region were observed [see Fig. 33(b)]. In some regions equiaxed dimples also occurred [Fig. 33(c)]. Thus it seems that although there are some fine discontinuous precipitates of carbides at the grain boundaries, they do not give rise to intergranular failure either in the low or high carbon tempered martensitic structures.

IV. DISCUSSION

A. Morphology of Martensite

Although considerable work has been done on the morphology of martensite in Fe-Ni, Fe-C and Fe-Ni-C steels; many features are not very clearly understood. A few points that are relevant to this work will be discussed here.

It is known[17,18,27,28] that with increasing nickel or carbon contents the morphology of martensite changes from lath [or the so-called massive martensite] to the twinned acicular martensite plates. This transition does not take place at any particular composition but over a composition range. Marder and Krauss[28] reported that in plain iron-carbon alloys only lath or massive martensite forms below 0.6% carbon. But in the present case even at 0.24% carbon isolated examples of twinning were observed. Speich and Warlimont[17] also observed some internally twinned martensite plates at 0.14% carbon in plain iron-carbon alloys. Thus if the massive martensite described by Marder and Krauss is taken to be identical with the lath martensite the demarkation at 0.6% carbon level does not appear tobe correct because twinned martensite plates can form much below 0.6% carbon.

There seems to be some doubt as to whether the adjacent martensite laths are twin related with respect to each other or not. Speich and Swann[27] observed twin related martensite laths in iron-nickel alloys, whereas Owen et al.[18] did not observe any. In low carbon steels Kelly and Nutting[16] observed twin related laths only in one case but Marder and Krauss[28] could not observe any. In the present investigation it was found that very frequently a group of martensite laths were separated by a high angle boundary from another group and were not twin-related,

and the individual laths in one group were separated from each other by low angle boundaries (Fig. 14). All these non-twin related laths were about 0.25μ in width. But when the cell width became about 1μ or bigger the adjacent laths became twin related (Fig. 13). The laths that Speich and Swann[27] observed to be twin related were also about 1μ in width. Thus it seems that when the cell width becomes larger the adjacent laths try to minimize their strain energy by becoming twin related. On the other hand when narrow laths form side by side they can accommodate their strain only with a slight misorientation. So it is most likely that whether adjacent laths will be twin related or not depends on their cell width.

When austenite transforms to martensite, strain energy associated with the transformation must be minimized. Based on this, Wechsler et al.[29] have shown that the interface plane (habit plane) separating the two phases must be one of zero average distortion and for this to be true, the transformation as a whole must in general be inhomogeneous. This pattern of inhomogeniety, sometimes referred to as "lattice invariant shear" can be either slip or twinning. The plate-like martensite formed at lower temperatures in more concentrated alloys are either partially or completely twinned whereas the martensite obtained in lower carbon or nickel alloys with $\{225\}_{\alpha}$ habit are partially twinned. The phenomenological theories of martensitic transformation have successfully accounted for these observed habits in the plate-like martensite, but the theories have not been adequately developed for lath martensite which is usually not twinned. From optical and electron microscopic observations in Fe-Ni alloys Patterson and Wayman[30] concluded that the plate-like martensite is associated with internal twins and if no twins are observed, the

martensite is not plate-like. In the present investigation many examples of internal twinning were found in the martensite which appeared more like narrow laths rather than plates. Also many multidirectional plates did not exhibit twinning. However the distinction between the laths and plates needs careful observation.

As mentioned before there have been many suggestions[12-14,31] that whether the martensite will be twinned or not depends on the temperature at which it forms. But it is known[32] that many alloys with very low M_s temperatures do not show much internally twinned martensite plates, where as others with a comparatively higher M_s temperature show considerable twinning. In the present case it has been shown that atsimilar M_s temperatures the martensite in a steel with a higher carbon (524) shows much more internal twinning than a steel with a lower carbon (142). The martensite formed in iron-nickel alloys with very low carbon exhibit a little or no internal twinning although at the same M_s temperature carbon containing steels show considerable internal twins. Thus it appears that increasing carbon promotes internal twinning in the martensite, apart from its effect in lowering the M_s and M_f temperature. This is in disagreement with the observations by Kelly and Nutting[16] who reported that the carbon content of the steel has only an indirect effect on the morphology of the martensite through its control of M_s and M_f temperatures. In simple binary alloys of Fe-Ni or Fe-C decreasing M_s temperature gives increasing internal twinning but at the same M_s temperature all of them will not have the same extent of twinning. The situation is further complicated when several other alloying elements such as Co, Cr are also present, in which case their influence on the occurrence of microtwins in the martensite cannot be predicted from their simple effect on M_s temperature.

The strain induced martensite that forms at room temperature in a Fe-23Ni-4Mo-0.28C alloy has been found to contain no internal twins,[32] although the martensite in the same steel obtained by quenching shows twinning.[33] During deformation the M_s temperature is raised to M_d and the A_s decreased to A_d and so the transformation hysteresis gap decreases. The area of the hysteresis loop of the martensitic transformation gives an indication of the driving force for the reaction which in turn may be related to the strain energy of the transformation. Intuitively, one can deduce that when there is a large strain energy or driving force (which is roughly indicated by the large hysteresis loop), the tendency of the martensite plate may be to be twinned rather than slipped. Thus the absence of internal twinning in the stress induced martensite could be a result of decreased driving force which can be roughly measured by the area of the hysteresis loop. Thus the influence of the various alloying elements on twinning in martensite can probably be understood by their effect on the area of the hysteresis loop. This includes the effect of the alloying elements both on M_s, M_f and A_s, A_f temperatures. Thus we can see why an iron-nickel alloy with the same M_s temperature as an iron-carbon alloy shows comparatively less twinning. It is because the area of the hysteresis loop for iron-carbon alloy is expected to be larger. At this stage it is not possible to say this definitely without experimental verification but we can expect it to be so. Because if M_s temperature is kept constant, increasing carbon content decreases only A_f and not A_s, whereas increasing the nickel content decreases both A_s and A_f. Hence if we increase the carbon and the nickel contents proportionately such that M_s temperature remains same in both cases, the areas of the hysteresis loop for Fe-Ni alloys will be smaller than the Fe-C alloys, assuming the slopes to remain roughly the same in both alloys.

B. Morphology of Bainite

The fact that in the lower bainite the carbides precipitate unidirectionally on {112} planes, instead of the {110} planes in the Widmanstatten morphology has led various investigators to believe that it must be precipitating on some kind of planar defect. Shackelton and Kelly[26] suggested that the bainitic ferrite that forms martensitically from austenite may be twinned and the cementite may subsequently precipitate on these twins. But they failed to detect the presence of any internal twins. They argued that by tempering the twins are removed and so during the isothermal holding they could also have been removed. Here it has been shown ealier that the internal twins in the martensite are not easily removed by tempering even at higher temperatures than the isothermal holdings temperature for bainite. So it is established that the inhomogeneous shear in the bainitic ferrite is not internal twinning. This is in agreement with the findings of other workers[34-36]. Shimizu et al. suggested that the ferrite that forms martensitically in the lower bainite may be accompanied by stacking faults and the cementite may form along the fault planes. But in view of the fact that stacking faults in bcc metals are rarely seen, this explanation seems to be very unlikely. The crystallographic observations on lower bainite in a Fe-8% Cr-1.1%C alloy by Srinivasan and Wayman[37] shows that the observed habit plane of bainite in this alloy is different from that of the martensite in the same alloy. Also they found that the internal twinning cannot explain the observed habit plane and the austenite-ferrite orientation relationship. Since the absence of internal twins in bainitic ferrite is established, the reason why the cementite precipitates on only {112} planes still remains to be answered.

It has been shown earlier that at lower transformation temperatures (in 0.4% carbon steels) the bainite form predominantly as plates, where as at higher transformation temperature (in 0.24% carbon steels), laths form side by side with a slight misorientation (Figs. 29 and 30). Oblak and Hehemann[36] observed such laths in the upper bainite but not in lower bainite.. But there is no reason why such laths should not form in the lower bainite if they are being formed at sufficiently higher temperatures. This is again analogous to the formation of martensite laths at high M_s temperatures as has been discussed in the previous section. This frequently observed side by side nucleated laths in the bainite of the various steels investigated suggests that the rate at which such substructural units nucleate may be important in controlling the growth rate of bainite, as has been proposed by Oblak and Hehemann[36].

The transition from lower to upper bainite is known[38] to take place around 650°F. But the structure observed in Fig. 30 for steel 143 transformed at 670° showed almost all lower bainite, as evidence by the characterisitc carbide morphology. Pickering[3] has shown that the maximum temperature above which no lower bainite forms depends on the carbon content of the alloy. According to his results this temperature is above 800°F for 0.24% carbon alloys. Thus it is not suprising that the transformation at 670°F gives almost all lower bainite in 0.24% carbon alloy.

C. Toughness of Tempered Martensite and Bainite.

The comparison of toughness between different structures such as tempered martensite and bainite are frequently at the same strength levels, as was done in the present case. Various strength levels in martensite were achieved by tempering at different temperatures. But the toughness of tempered martensite does not always increase continuously with increasing

tempering temperature. In many high strength steels the so-called 500°F embrittlement is observed when tempering in the 400-700°F range. This has been associated with the resolution of ϵ-carbide and simultaneous precipitation of cementite and the following explanation has been given.[20] The formation of cementite from ϵ-carbide does not take place in situ, which is clear from the simple observation that ϵ-carbide did not precipitate preferentially on the twin boundaries whereas the cementite did. When this more stable carbide precipitates, it is precipitated at dislocation intersections and jogs. Thus, precipitate locked dislocation intersections and jogs, along with high dislocation densities give rise to a lower notch toughness. But in the present case the embrittlement was observed in almost all the cases around 800°F which is above the range of 400°F-700°F. Moreover, it was observed that tempering at 400°F gives mainly ϵ-carbide in 0.4% carbon steels and at 800°F mainly Fe_3C. But in 0.2% carbon steels ϵ-carbide started to dissolve at still lower temperature than 400°F. This means that the resolution of ϵ-carbide and the precipitation of Fe_3C has occurred in between this range. So it is rather difficult to say if the observed embrittlement can be associated with the 500°F embrittlement. During the comparisons between various structures at the same strength levels, this embrittled range was avoided as far as possible. The observed toughness difference between the various structures can now be related with the observed structural differences. The following factors appear to be important in controlling the toughness of the various structures.

1. Twinning

The mechanical test results have established that at equivalent strength levels the toughness of lower bainite structure is not always

superior to the tempered martensitic ones. Only in the 0.4% carbon steels which exhibited considerable twinning did the martensite show poor toughness compared to the bainitic structures, which did not exhibit any twinning. The martensite of 0.24% carbon steels which showed a small amount of twinning possessed a very high toughness, compared to both the internally twinned martensite and bainite with no twins. Thus, the role of internal twins in lowering toughness has been demonstrated in two ways. Firstly the comparison between heavily twinned and the mainly untwinned martensite shows superior toughness of the latter. Secondly, when the martensite is twinned the corresponding twin free bainite shows a higher toughness, but when the martensite does not show any twinning, it has better toughness than the bainite. In this second case the difference in the toughness between bainite and tempered martensite lies in the distribution of the carbides and the arrangement of the plates, which will be discussed in the next section.

As we have seen before, in the presence of twins the cementite precipitates preferentially all along the twin boundaries. Thus the carbides are much longer than if they had precipitated in a twin free matrix. These long precipitates of carbides allow a twin boundary to act as a strong barrier for dislocations to pile up rapidly and nucleate cleavage cracks. Also in the presence of internal twins in the martensite, the slip is very much restricted and the deformation mode is mechanical twinning. Krauss and Pitsch[39] have shown that the deformation twins can occur in the martensite plate having fine transformation twins. Also Richman[40] has shown that slip occurs in the martensite up to about 0.4% carbon; beyond which mechanical twinning becomes effectively the only plastic deformation mode. This is consistent with the present observations that at and above 0.4% C the martensite will show considerable transformation

twins in which case the deformation mode is likely to be mechanical twinning. It is well known[41] that twin intersections are very favorable sites for the nucleations of cleavage cracks. Thus it is seen that the presence of internal twins in the martensite plates is the major factor responsible for its lower notch toughness.

2. Size and Distribution of Ferrite and Carbide

The ferrite grain size is very important in controlling the toughness.[42] The smaller the ferrite grain size the greater is the energy absorbed during cleavage. In the present case the ferrite lath size in the martensite and bainite was found to be very nearly the same. So their contribution to the toughness is nearly the same in both cases.

In the 0.24% steels the martensite consists of a mixture of laths and multidirectional plates, whereas the bainite in the same steels shows predominantly laths. As mentioned before these laths are separated by low angle boundaries. So the fracture path will be easier in these laths compared to multidirectionally arranged plates, inside an austenite grain. Because in the latter case the fracture path has to change directions frequently in going from one grain to the other and so it will be tortured and this will absorb more energy. This can be one of the factors responsible for the lower toughness of the higher temperature bainites in low carbon steels compared to the martensite. So the bainite or the martensite formed at higher temperatures, which show higher proportion of laths should have poor toughness compared to the ones that have multidirectional plates. This is very true for the case of bainite as has been shown but not for martensite. In this martensite the presence of internal twins in the plates over-rides this effect and lowers their toughness. This further emphasizes the importance of internal twins in

the martensite plates in lowering the toughness.

The size and distribution of carbides is also important in controlling the toughness. In the twin free regions of martensite fine carbides are precipitated in the Widmanstatten pattern. Here the crack propagating through a particular ferrite grain cannot avoid the carbide particles [Fig. 24(d)]. This is the predominant structure of the 0.24% carbon martensites, which show very high toughness values. The structure of bainites in the same steels (e.g. Fig. 29), shows very few, relatively coarse carbides here and there in one direction only. So the fracture path may not meet any carbides. Thus the latter structure will offer a relatively lower resistance to fracture than the former. This explains why the lower bainite in these 0.24% carbon steels have lower toughness than the corresponding tempered martensites.

It is commonly observed that a decrease in volume fraction of the hard second phase helps in increasing the toughness. Obviously the volume fraction of the carbide is higher for the higher carbon contents, which contributes to the lower toughness. Although the detailed estimate of volume fractions of the carbides have not been made for the bainitic and tempered martensitic structures, they do not appear to be greatly different. However, in the lower bainite isothermally transformed at higher temperatures the volume fraction of carbides may be slightly higher which may contribute to their lower toughness.

3. Grain Boundary Carbides

The presence of precipitate at the grain boundaries is one of the well known reasons for lowering of toughness and causing intergranular failure. It is very difficult to avoid such grain boundary precipitation of carbides. If the precipitates are continuous all along the grain

boundary they help in nucleation of cracks by acting as strong barriers to dislocation motion and transfer of plastic strain from grain to grain. The grain boundary carbides were prominant in martensite only on tempering at higher temperatures and in bainite transformed at higher temperatures. Since intergranular failure was apparently not observed, the fine discontinuous carbides at the lath or plate boundaries were not very effective to cause intergranular failure, although some weakening of the boundary is always there. This weakening effect can be taken to be more or less the same while comparing the different martensites tempered at relatively lower temperatures. The grain boundary carbides in the bainites formed at 600°F in higher than 0.4% carbon steels may also be somewhat responsible for their lower toughness compared to the 500°F bainite, in addition to the previously mentioned factors.

D. Design of Alloys

The majority of commercially used alloys have been designed by trial and error. With a better and better understanding of the microstructure, it is becoming increasingly possible to redesign the alloys from more fundamental considerations. Usually one aims to achieve a high toughness at a given strength level. The addition of carbon is helpful in achieving high strength levels in the quenched and tempered steels, but their excessive use is prohibitive because of the increased twinning in martensite which severely impairs the toughness. In such high carbon steels, the trend should be to go for a fully lower bainitic structure to get better toughness. Again it is important to see whether a fully bainitic structure can be obtained or not. The presence of virgin martensite, which severely impairs the strength and toughness should be completely avoided, because the martensitic areas are neither sufficiently fine nor

sufficiently dispersed to act as efficient barriers to the propagation of cleavage cracks. On the other hand at lower carbon levels the quenched and tempered structures are the most desired ones rather than the bainitic structures. One of the aims of this work was to see if it is possible to find some design parameter such as M_s temperature of the alloy which can control the extent of internal twins in the martensite and hence its toughness. As seen earlier in the simple binary alloys like Fe-C or Fe-Ni etc. this may be possible. But in the presence of several alloying elements, which is most often the case, this is not possible. If some suitable parameters could be found that give a good indication of the extent of internal twinning in martensite, it may be possible to design alloys on that basis. The area of the hysteresis drop during the martensitic transformation may be one such parameter.

V. CONCLUSIONS

1. At similar M_s temperatures the structure of martensite in a steel containing higher carbon exhibits greater amount of internal twinning than the low carbon ones. Thus carbon content has an influence in promoting internal twinning in the martensite, in addition to its effect on M_s temperature.

2. Although in simple binary Fe-C or Fe-Ni alloys M_s temperature can give some indication of the extent of internal twinning in martensite, it fails when there are two or more alloying elements. It is suggested that the area of the hysteresis loop of the transformation may give a better indication of occurence of twinning. The larger the area, the greater is the tendency for the martensite to twin.

3. The narrow martensite laths of about 0.25μ width which form within a group, are separated from each other by low angle boundaries. The relatively wider ones of about 1μ or greater tend to be twin related with respect to each other.

4. The ferrite in lower bainite shows no internal twinning at all. At lower transformation temperature ferrite is predominantly plate-shaped, but the proportion of laths increase with increasing transformation temperature.

5. At similar yield and ultimate tensile strength levels all the 0.24% carbon steels showed higher toughness than the 0.4% carbon steels. The toughness difference is primarily due to the difference in the extent of internal twinning in the two structures. Increased amount of twinning

in the high carbon steels reduces its toughness.

6. On increasing the isothermal transformation temperature, the strength and toughness of the bainite decrease. The decrease in toughness is mainly due to the carbide particle coarsening and its precipitation at the grain boundaries.

7. The toughness of lower bainite transformed at low temperatures is higher than the tempered martensite, that shows excessive twinning, when compared at equivalent yield and tensile strength levels.

8. The toughness of lower bainite is not higher than the tempered martensite that shows very little internal twinning. This difference is mostly due to the fact that in these twin free martensites the fine carbides precipitate in a Widmanstatten pattern, where as in lower bainite small, slightly coarser carbides precipitate in only one direction.

9. The mechanical properties of incompletely transformed bainite are very poor because of the presence of virgin martensite.

10. The addition of cobalt promotes autotempering by raising M_s temperature. The autotempered precipitates is Fe_3C in 0.24% carbon steels.

11. The addition of cobalt in excess of 4% decreases the toughness.

ACKNOWLEDGEMENTS

The author is deeply grateful to Professor Gareth Thomas for his personal guidance, encouragement and support throughout the course of this work. He is also thankful to the Republic Steel Corporation for supplying the alloys and to the staff of its research center for helpful discussions.

Special thanks are due to Mr. W. W. Gerberich for valuable suggestions and help during the course of this work.

This work was done under the auspices of the U.S. Atomic Energy Commission through the Inorganic Materials Research Division, of the Lawrence Radiation Laboratory.

REFERENCES

1. J. S. Pascover and S. J. Matas: ASTM special Publication No. 370 (1965).

2. K. J. Irvine and F. B. Pickering - J. Iron and Steel Inst. 201 518 (1963).

3. F. B. Pickering in symposium: Transformation and Hardenability in Steels, Climax Molybdenum Co. (1967).

4. E. S. Davenport, E. L. Roff and E. C. Bain: Trans ASM 22, 289 (1934).

5. B. J. Waterhouse: Discussion, "Physical Properties of Martensite and Bainite", special Report 93, The Iron and Steel Institute (London), 147 (1965).

6. L. J. Klinger, W. J. Barnett, R. P. Frohmberg and A. R. Troiano, Trans. ASM 46, 1557 (1954).

7. R. F. Hehemann, V. J. Luhan, and A. R. Troiano, Trans ASM 49 409, (1957).

8. S. A. Herres and C. H. Lorig, Trans ASM 40, 775 (1948).

9. G. Sachs, L. J. Ebert, and W. F. Brown, Trans AIME 176, 424 (1948).

10. J. H. Hollomon, L. D. Jaffe, D. E. McCarthy and M. R. Norton, Trans ASM, 38, 807 (1947).

11. A. S. Tetelman, Discussion, "High Strength Materials". Ed. V. F. Zackay, John Wiley an Sons, New York (1965), 324.

12. P. M. Kelly and J. Nutting, J.Iron and Steel Inst. 197, 199 (1961).

13. O. Johari and G. Thomas, Acta. Met., 13, 1211 (1965).

14. R. L. Patterson and C. M. Wayman, Acta Meta. 12, 1306 (1964).

15. J. S. Pascover and S. J. Matas in Fourth Maraging Steel Project Review, WADC Technical Documentary Report No. ML-TDR-64-225 (1964).

16. P. M. Kelly and J. Nutting, Proc. Roy. Soc. (A), 259, 45 (1960).

17. G. R. Speich and H. Warlimont, J. Iron and Steel Inst., 206, 385 (1968).

18. W. S. Owen, E. A. Wilson and T. Bell, in High Strength Materials, ed., V. F. Zackay, John Wiley and Sons, New York, 167 (1965).

19. E. W. Page, P. Mangonon, G. Thomas and V. F. Zackay, submitted to Trans. ASM, UCRL-18386.

20. B. R. Banerjee, J. Iron and Steel Inst. 203, 166 (1965).

21. H. Warlimont, private communication.

22. M. G. H. Wells, Acta Met. 12, 389 (1964).

23. E. Tekin and P. M. Kelly, in Precipitation from Iron-Base Alloys, eds., G. R. Speich and J. B. Clark, Gordon and Breach Science Publishers, New York (1965).

24. A. J. Baker, P. M. Kelly and J. Nutting, in Electron Microscopy and Strength of Crystals, eds. G. Thomas and J. Washburn, John Wiley and Sons, New York (1963).

25. Second progress report by Subcommittee XI of Committee E-4, Electron Microstructure of Bainite in Steel, ASTM Proc. 52, 543 (1952).

26. D. N. Shackleton and P. M. Kelly, The Iron and Steel Inst., (London) Special Report 93, 126 (1965).

27. G. R. Speich and P. R. Swann, J. Iron and Steel Inst. 203, 480 (1965).

28. A. R. Marder and G. Krauss, Trans. ASM 60, 651 (1967).

29. M. S. Wechsler, D. S. Lieberman and T. A. Read, Trans. AIME, 197, 1503 (1953).

30. R. L. Patterson and C. M. Wayman, Acta Met., 14, 347 (1966).

31. R. F. Vyhnal and S. V. Radliffe, Acta Met., 15, 1475 (1967).

32. K. Shimizu and C. M. Wayman, Acta Met., 14, 1390 (1966).

33. J. A. Hall, M.S. Thesis, University of California, Berkeley: UCRL-18282, 1968.

34. O. Johari and G. Thomas, Trans. ASM 58, 563 (1965).

35. K. Shimizu, T. Ko and Z. Nishiyama, Trans. Japan Inst. of Metals 5, 225 (1964).

36. G. R. Srivivasan and C. M. Wayman, Acta Met. 16, 609 (1968).

37. J. M. Oblak and R. F. Hehemann in Symposium: Transformation and Hardenability in Steels, Climax Molybdenum Co., 15, (1967).

38. G. R. Srinivasan and C. M. Wayman, Acta Met. 16, 621 (1968).

39. S. J. Matas and R. F. Hehemann, Trans. AIME 221, 179 (1961).

40. G. Krauss and W. Pitsch, Acta Met. 12, 278 (1964).

41. R. H. Richman, Trans. AIME, 227, 159 (1963).

42. D. Hull, Acta Met., 8, 11 (1960).

43. J. R. Low, in Fracture, eds. B. L. Averbach et al., M.I.T. Press, John Wiley and Sons, New York, (1959).

TABLE I.

Chemical Composition of the Alloys With Their M_s Temperatures

Heat No.	C	Mn	Si	Cr	Mo	V	Ni	Co	M_s Temp. °F
140	.24	.32	.11	.50	.51	.084	4.9	4.0	700
141	.24	.33	.086	.48	.49	.083	8.4	3.9	590
142	.24	.31	.053	.44	.48	.086	12.5	3.8	498
143	.24	.34	.13	.57	.49	.084	5.2	0.52	640
145	.24	.31	.094	.44	.44	.075	11.3	7.5	584
522	.43	.40	.14	.52	.54	.087	8.6	3.97	436
523	.39	.38	.10	.50	.54	.087	11.95	4.0	286
524	.40	.40	.15	0.52	0.57	0.09	8.3	7.2	486

TABLE II

Mechanical Properties of Tempered Martensitic Structures*

Heat No.	Tempering Temperature °F	Y.S. $\times 10^3$ psi (0.2% off set)	UTS $\times 10^3$ psi	% Elongation	K, KSI-IN$^{1/2}$ at -196°C
140	1000	166	176	13.3	51.05
141	400	176.7	207	9.8	135.0
	600	175.5	195.6	9.0	118.7
	800	172.2	183	10.17	97.75
	1000	175	182	11.85	115.4
142	400	173	203	9.35	158.2
	600	175.4	194.6	10.3	139.7
	800	173.5	186.3	11.91	126.5
	1000	175.2	180.7	12.7	139
143	400	175.3	205.2	9.26	60.9
	600	172.3	191.6	8.78	65.1
	800	163	173.9	8.53	70.98
	1000	161.2	170.5	12.1	52.6
145	400	172.0	204.0	9.5	139.3
	600	172.5	194.9	9.62	123.7
	800	174.3	187	10.77	47.5
	1000	176.2	181.9	12.13	101.35
522	400	226.0	266.4	8.48	40.1
	600	216.7	243.2	7.25	46.4
	800	192.5	224.3	9.28	38.05
	1000	191.3	215.5	10.0	64.8
	1100	194.3	211.8	9.76	74.6
523	400	229	266	8.08	43.5
	600	208.6	242.2	8.88	43.85
	800	194	230	10.4	36.58
	1000	190	214	11.42	63.8
	1100	185.4	211.3	11.80	68.15
524	400	251	288	6.78	35.6
	600	237.5	267	6.84	33.9
	800	214.5	240.2	7.64	29.3
	1000	200.1	224.3	8.13	39.2
	1200	184.3	195.1	8.91	

*Double Tempered at each temperature for 2 + 2 hours.

TABLE III

Mechanical Properties of Bainitic Structures

Heat No.	Isothermal Transformation Temperature °F	Transformation Time in hours	Tempering * Temperature °F	Y.S. $\times 10^3$ psi (0.2% off set)	U.T.S. $\times 10^3$ psi	Elongation	Kat -196°C Ksi - $in^{1/2}$
141	620	24		146.4	188.2	11.35	54.6
	620	24	1000	173.56	186	12.95	56.8
143	680	24		138.4	164.8	10.32	46.2
	680	24	1000	152.3	163.9	14.6	44.25
145	620	24		135.2	200.3	12.32	54.1
	620	24	1000	176.8	191.9	13.6	73.1
522	500	24		188	232.3	10.6	50.5
	620	28		169.0	212.0	11.3	32.6
	500	24	1000	183.0	198.5	12.1	49.2
524	550	24		205.4	237.8	7.88	35.7
	550	24	1000	202.0	219.5	8.72	32.6
	600	24		181.5	229.0	6.9	34.1

*Double tempered at each temperature for 2 + 2 hours

TABLE IV

Comparative Toughness Values of Tempered Martensitic and Bainitic Structures at Similar Strength Levels

Heat No.	Strength Level Ksi	K at 25°C Ksi-in$^{1/2}$		K at -196°C Ksi-in$^{1/2}$	
		Tempered Martensite	Bainite	Tempered Martensite	Bainite
141	Y.S. ~ 173	-	-	102	56.8
	UTS ~ 186	-	-	98	56.8
145	Y.S. ~ 177	-	-	111	73.1
	UTS ~ 192	-	-	93	73.1
522	Y.S. ~ 190	-	-	44	50.5
	UTS ~ 230	66.5	90.2	41.5	50.5
524	Y.S. ~ 205	54.2	82	33.5	35.7
	UTS ~ 238			30	35.7

FIGURE CAPTIONS

Figure 1. The dimensions of mechanical test specimens.

Figure 2. The effect of tempering temperature of the strength and toughness of steel 522.

Figure 3. The effect of tempering temperature on the strength and toughness of steel 523.

Figure 4. The effect of tempering temperature on the strength and toughness of steel 524.

Figure 5. The effect of tempering temperature on the strength and toughness of steel 141.

Figure 6. The effect of tempering temperature on the strength and toughness of steel 142.

Figure 7. The effect of tempering temperature on strength and toughness of steel 145.

Figure 8. Comparison of notch toughness (K) of various steels at different yield strength levels.

Figure 9. Comparison of notch toughness (K) of various steels at different ultimate tnesile strength levels.

Figure 10 Transmission electron micrograph of martensite of steel 140. (a) the martensite laths nucleated on either side of the prior austenite grain boundary. The laths near A and B are in [111] and [100] orientations respectively. (b) and (c) show auto-tempered precipitates of Fe_3C with {110} habit.

Figure 11 Structure of martensite in steel 142 showing (a) martensite lath (b) small amount of internal twins in a plate.

Figure 12 Twinned and untwinned regions of martensite of steel 143. (a) Uneven distribution of twins which reverse contrast in

the dark field micrograph in (b). (c) small twins restricted to the area near the edge of the plate (d) another region showing very little internal twins.

Figure 13 Martensite in steel 145 (a) Internal twins in the midrib at A. (b) Dark field of the $(0\bar{1}1)_T$ reflection from the selected area diffraction pattern in (c) shows reversal of contrast for the twins and the lath B. This proves that lath A and B are twin related. (d) Another region showing some possible fine internal twins in some of the narrow laths.

Figure 14 Structure of martensite is steel 145. (a) Groups of parallel laths (b) Selected area diffraction pattern of the circled area in (a), showing two b.c.c. orientations [100] and [111]. (c) Dark field of spot A reverses the contrast for the group of laths in [111], (d) Dark field of spot B shows only the laths in [100] orientation.

Figure 15 Martensite of steel 522 showing in (a) an extensively twinned region and in (b) twinned plates of various sizes.

Figure 16 (a) Bright field micrograph of martensite in steel 523 showing internal twinning (b) Dark field of spot A shows the twins clearly and also reverses the contrast for the adjacent plate, which are twin relaxed. (c) Selected area diffraction pattern showing extra spots due to double diffraction, and streaks in the $\langle 112 \rangle$ direction. (d) Indexed diffraction diffraction pattern.

Figure 17 (a) High density of twins in the midrib of martensite plate in steel 523. (b) Dark field of the streak (see inset) reverses contrast for the twins. (c) Another region showing slightly thicker twins.

Figure 18 Martensite of steel 524. (a) A high magnification micrograph showing high dislocation density and the internal twins Figs. (b) and (c) show varying amounts of twins in different regions.

Figure 19 Martensite of steel 522 double tempered at 400°F for 2+2 hours (a) Bright field micrograph showing internal twinning and fine precipitates of ϵ-carbide (b) Dark field reveals the internal twins clearly. (c) Precipitates of ϵ-carbide in a twin free region (d) Dark field of the same area as in (c) showing ϵ-carbides of one family. (e) Bright field of another region showing ϵ-carbides of two families (f) Dark field shows clearly that some Fe_3C of {110} habit has also begun to form at A.

Figure 20 Tempered martensite of steel 524 (800°F for 2 + 2 hours). (a) Precipitates of Fe_3C in a twin free region (b) Dark field of the same area as in (a). (c) Cementite precipitates at the twin boundaries and also along the grain boundary. (d) Dark field of same area as in (c) showing the reversal of contrast for Fe_3C precipitates at the twin boundaries.

Figure 21 Martensite of steel 522 tempered at 1100°F for 2 + 2 hours. (a) Precipitation of cementite at the twin boundaries and also at the grain boundaries. (b) Another region showing clearly the presence of twins which are brought to better contrast by tilting as in (c). (d) A twin free region showing spherodization of cementite precipitates.

Figure 22 (a) Martensite of steel 141 tempered at 400°F for 4 hours showing mainly precipitates of Fe_3C. (b) Martensite of steel 145 tempered at 600°F for 4 hours showing Widman-statten precipitates of only Fe_3C.

Figure 23 Structure of tempered martensite of steel 142 after tempering for 4 hours at 1000°F. (a) The cementite has precipitated at the plate boundaries which can be clearly seen in the dark field micrograph in (b) (c) A twinned region with cementite precipitated at the twin boundaries.

Figure 24 Martensite of steel 143 tempered at 1000°F for 4 hours (a) A twinned region showing fine precipitates of Fe_3C (b) Dark field taken from the twin reflection showing reversal of contrast for the twins (c) Discontinuous precipitates of carbides at the lath boundaries. (d) Another twin free region showing Widman-statten precipitation of cementite.

Figure 25 Lower bainite in steel 522 after isothermal transformation at 500°F for 24 hours. (a) An extensive bainite plate with cementite in it. (b) Dark field taken from the cementite reflection. (c) Another region showing side by side nucleated ferrile laths.

Figure 26 Lower bainite in steel 522 obtained by isothermal transformation at 550°F for 4 hours. (a) Carbides of varying sizes are seen due to sectioning effect. (b) Another region showing the typical lower bainite structure with carbides at an angle to the long direction of ferrite laths. Notice that carbides are coarser as compared to Fig. 25.

Figure 27 Lower bainite in steel 522 formed at 600°F after transforming for 24 hours. (a) Small carbides have precipitated at the boundaries, an addition to the ones inside the laths. These carbides reverse contrast in the dark field as in (b). (c) Another region showing coarse carbides at the plate boundaries. (d) Dark field of the same area as in (c).

Figure 28 Structure of lower bainite in steel 524 after isothermal transformation at 550°F for 24 hours. (a) Precipitates of carbides in an extensive ferrite matrix (b) Another region showing the classical lower bainite structure. (c) Same lower bainite structure showing rather long carbides.

Figure 29 Lower bainite in steel 141 obtained by isothermal transformation at 620°F for 24 hours (a) Bright field micrograph showing ferrite laths with small internal carbides (b) Dark field of $(1\bar{1}0)$ reflection showing reversal of contrast for the alternate laths.(c) Selected area diffraction pattern of the circled area in (a) showing the group of laths to in [111] orientation.

Figure 30 Lower bainite in steel 143 after isothermal transformation at 670°F for 24 hours. (a) Bright field micrograph showing ferrite laths nucleated on either side of the prior austenite grain boundary. [If Fig. 10(a)] (b) Dark field of $(1\bar{1}0)$ reflection in the SAD as in (c), showing alternate laths to be in the same orientation.

Figure 31 Electron fractograph of martensite of steel 142 tempered at 400°F for 4 hours, showing typical ductile failure.

Figure 32 Electron fractographs of martensite of steels 522 tempered for 4 hours at (a) 400°F (b) 800°F (c) 1000°F.

Figure 33 Electron fractograph of lower bainite of steel 522 after isothermal transformation at 500°F for 24 hours showing (a) quasi-cleavage facets (b) elongated dimples and (c) equiaxed dimples.

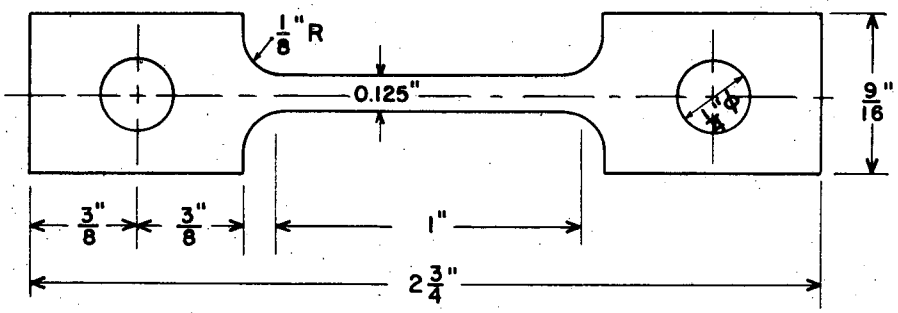

(a) TENSILE SPECIMEN, THICKNESS = 0.06".

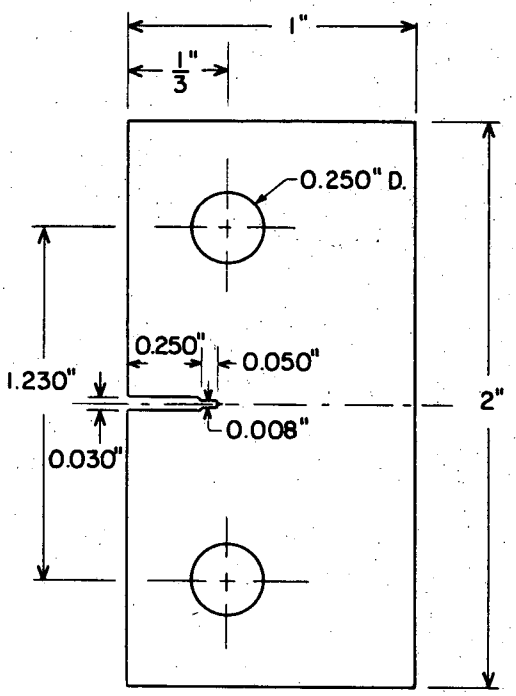

(b) SINGLE EDGE NOTCH FRACTURE SPECIMEN, THICKNESS = 0.06", TOTAL CRACK LENGTH ≈ 1/3".

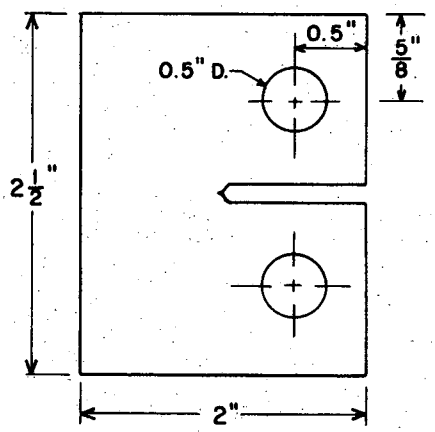

(c) SINGLE EDGE NOTCH FRACTURE SPECIMEN, THICKNESS = 1/2".

XBL 6811-6182

Figure 1

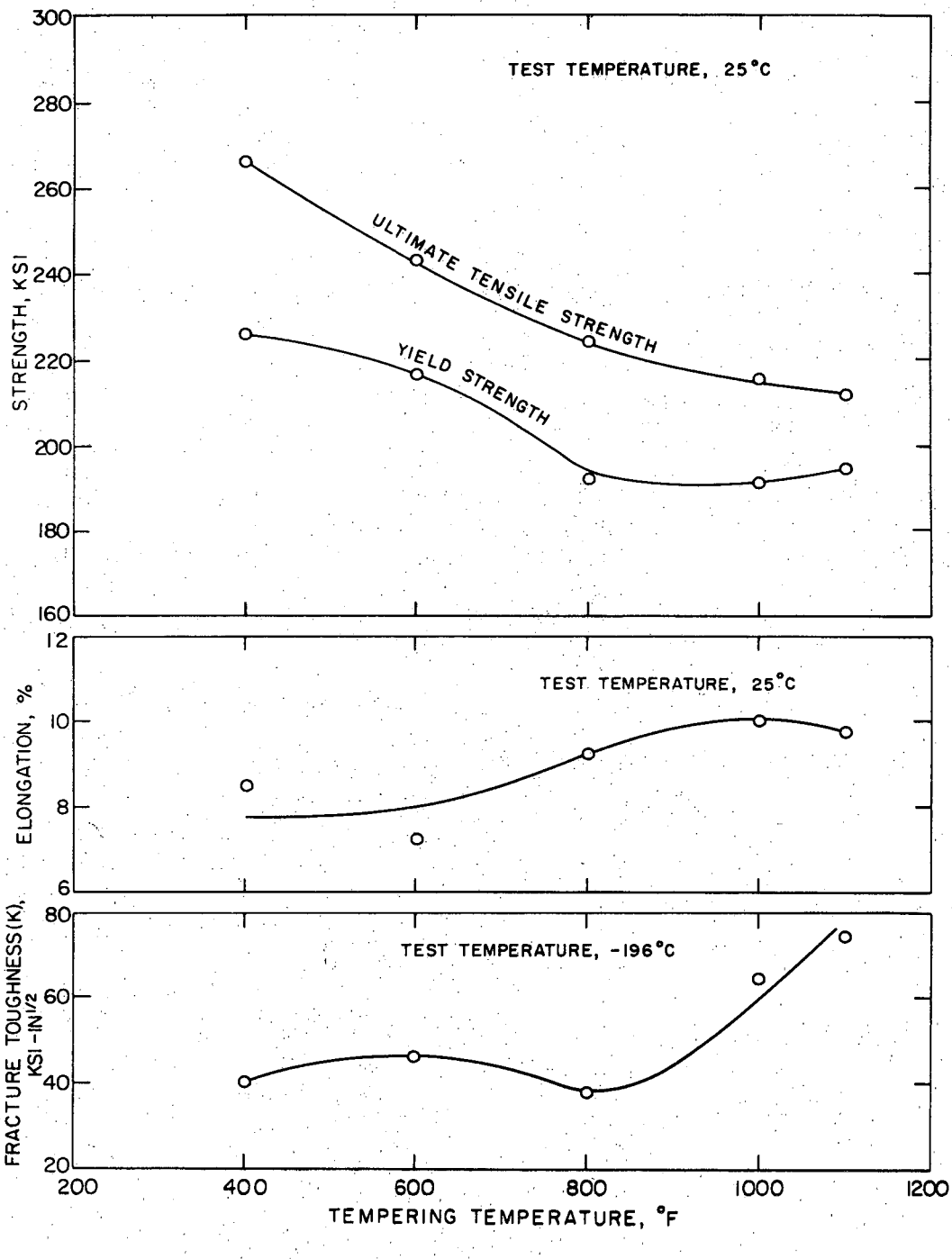
TEST TEMPERATURE, 25°C
ULTIMATE TENSILE STRENGTH
YIELD STRENGTH
STRENGTH, KSI
300
280
260
240
220
200
180
160
TEST TEMPERATURE, 25°C
ELONGATION, %
12
10
8
6
TEST TEMPERATURE, -196°C
FRACTURE TOUGHNESS (K), KSI-IN1/2
80
60
40
20
200
400
600
800
1000
1200
TEMPERING TEMPERATURE, °F
XBL 6811-6186

Figure 2

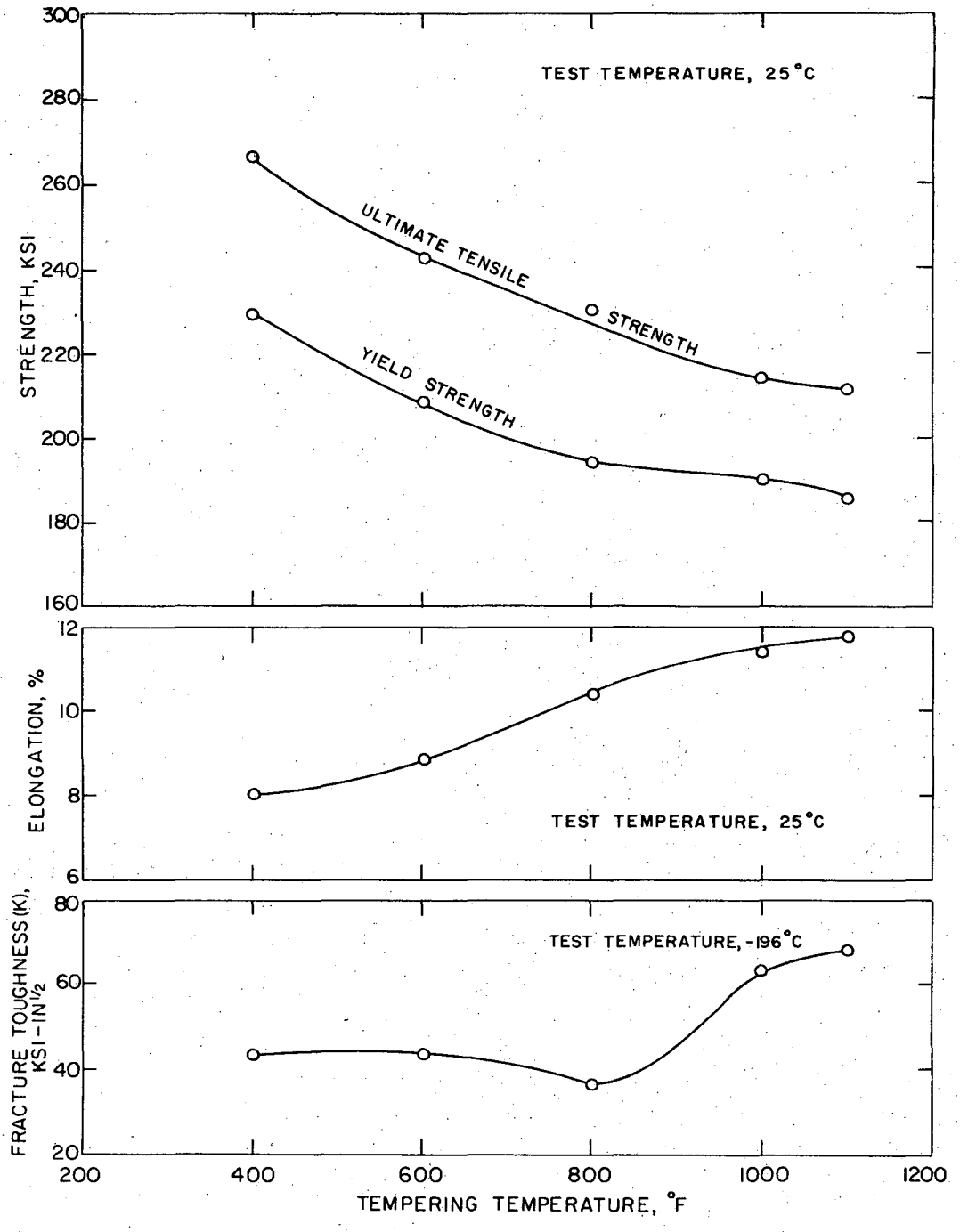
TEST TEMPERATURE, 25°C
ULTIMATE TENSILE STRENGTH
YIELD STRENGTH
STRENGTH, KSI
300
280
260
240
220
200
180
160
ELONGATION, %
12
10
8
6
TEST TEMPERATURE, 25°C
FRACTURE TOUGHNESS (K), KSI-IN$^{1/2}$
80
60
40
20
TEST TEMPERATURE, -196°C
200
400
600
800
1000
1200
TEMPERING TEMPERATURE, °F
XBL 6811-6187

Figure 3

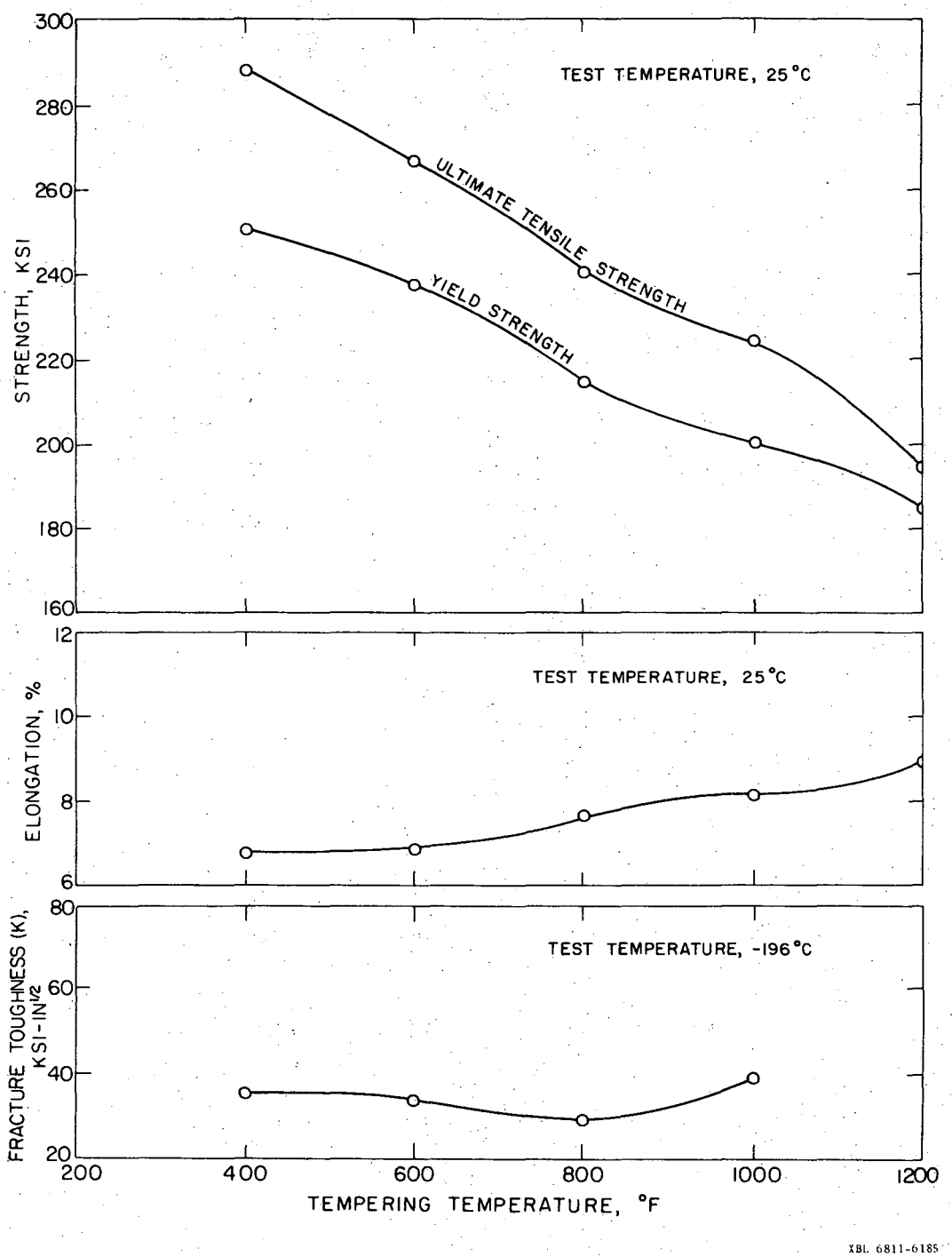
TEST TEMPERATURE, 25°C
ULTIMATE TENSILE STRENGTH
YIELD STRENGTH
STRENGTH, KSI
300
280
260
240
220
200
180
160
TEST TEMPERATURE, 25°C
ELONGATION, %
12
10
8
6
TEST TEMPERATURE, -196°C
FRACTURE TOUGHNESS (K), KSI-IN½
80
60
40
20
200
400
600
800
1000
1200
TEMPERING TEMPERATURE, °F
XBL 6811-6185

Figure 4

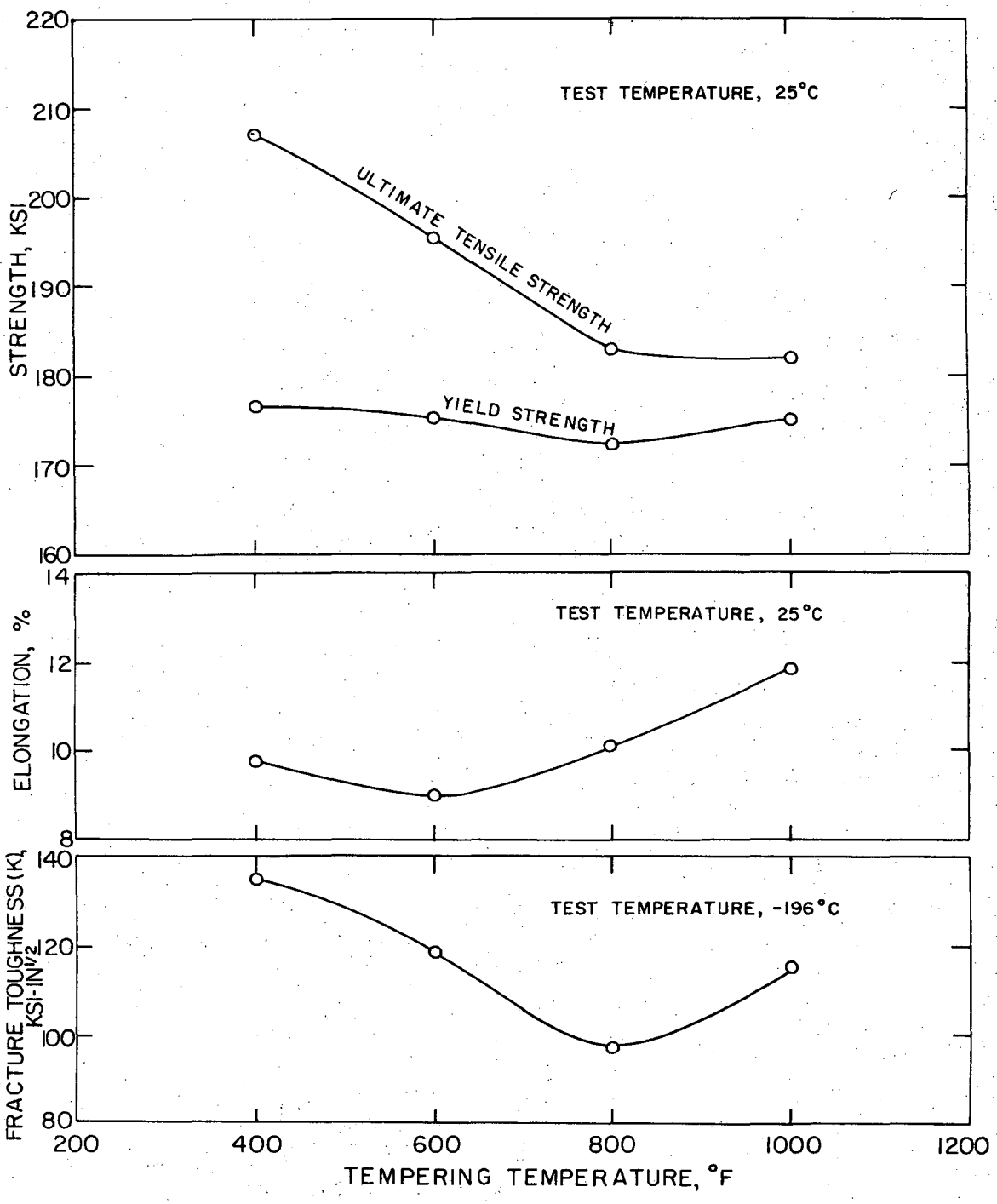

XBL 6811-6188

Figure 5

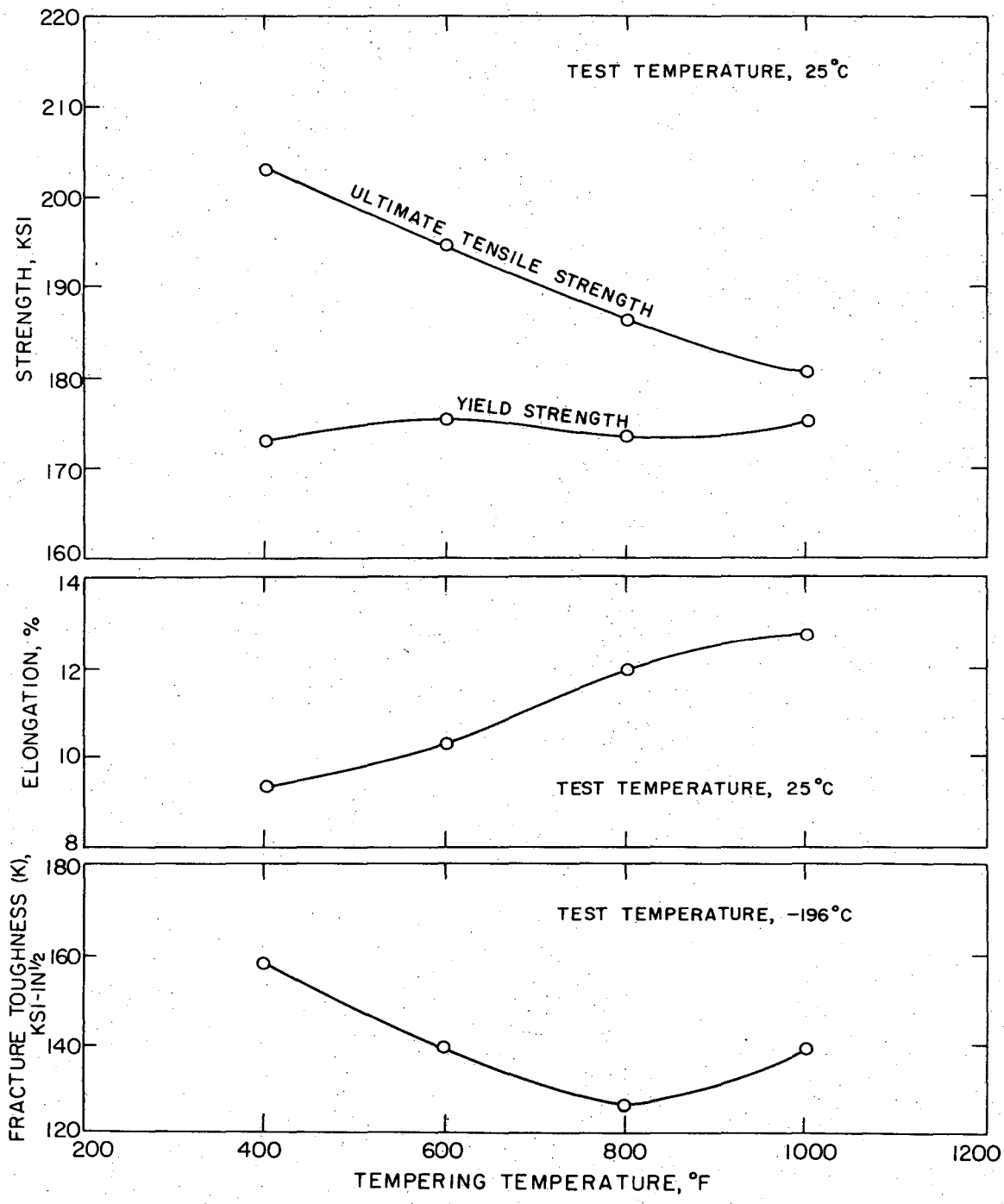
TEST TEMPERATURE, 25°C
ULTIMATE TENSILE STRENGTH
YIELD STRENGTH
STRENGTH, KSI
220
210
200
190
180
170
160
ELONGATION, %
14
12
10
8
TEST TEMPERATURE, 25°C
FRACTURE TOUGHNESS (K), KSI-IN½
180
160
140
120
TEST TEMPERATURE, -196°C
200
400
600
800
1000
1200
TEMPERING TEMPERATURE, °F
XBL 6811-6184

Figure 6

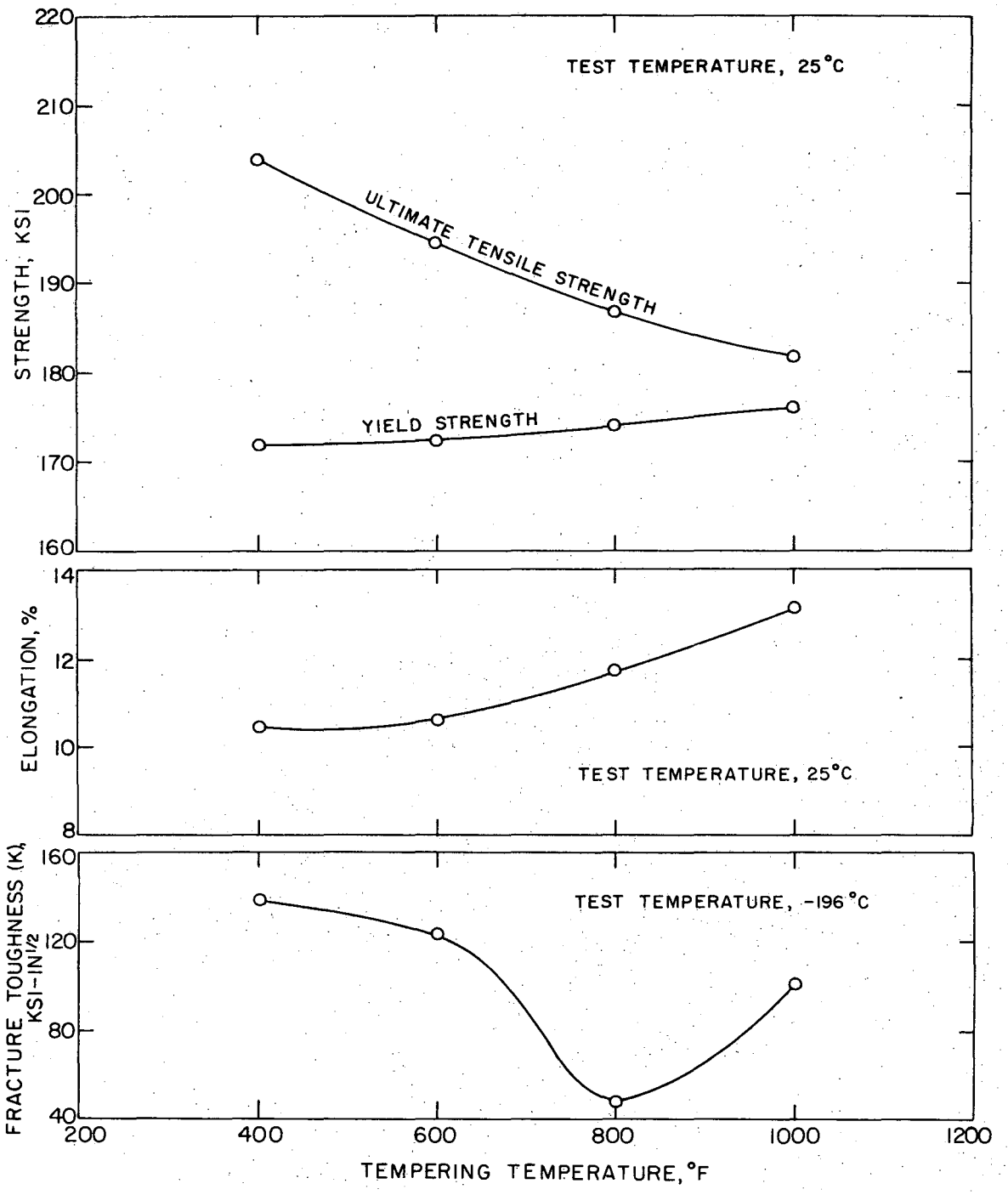
TEST TEMPERATURE, 25°C
ULTIMATE TENSILE STRENGTH
YIELD STRENGTH
STRENGTH, KSI
220
210
200
190
180
170
160
ELONGATION, %
14
12
10
8
TEST TEMPERATURE, 25°C
FRACTURE TOUGHNESS (K), KSI-IN1/2
160
120
80
40
TEST TEMPERATURE, -196°C
200
400
600
800
1000
1200
TEMPERING TEMPERATURE, °F
XBL 6811-6183

Figure 7

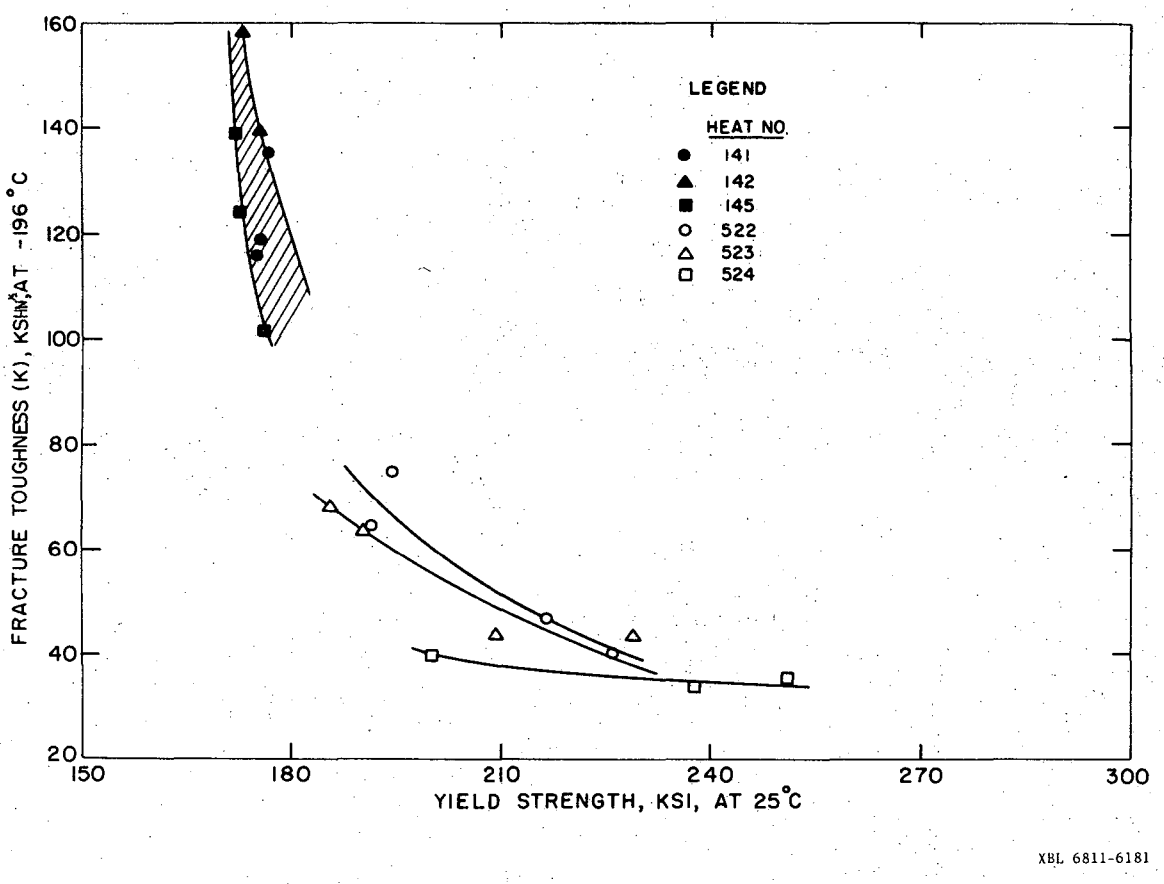
LEGEND
HEAT NO.
141
142
145
522
523
524
FRACTURE TOUGHNESS (K), KSI√IN, AT -196 °C
YIELD STRENGTH, KSI, AT 25°C
160
140
120
100
80
60
40
20
150
180
210
240
270
300
XBL 6811-6181

Figure 8

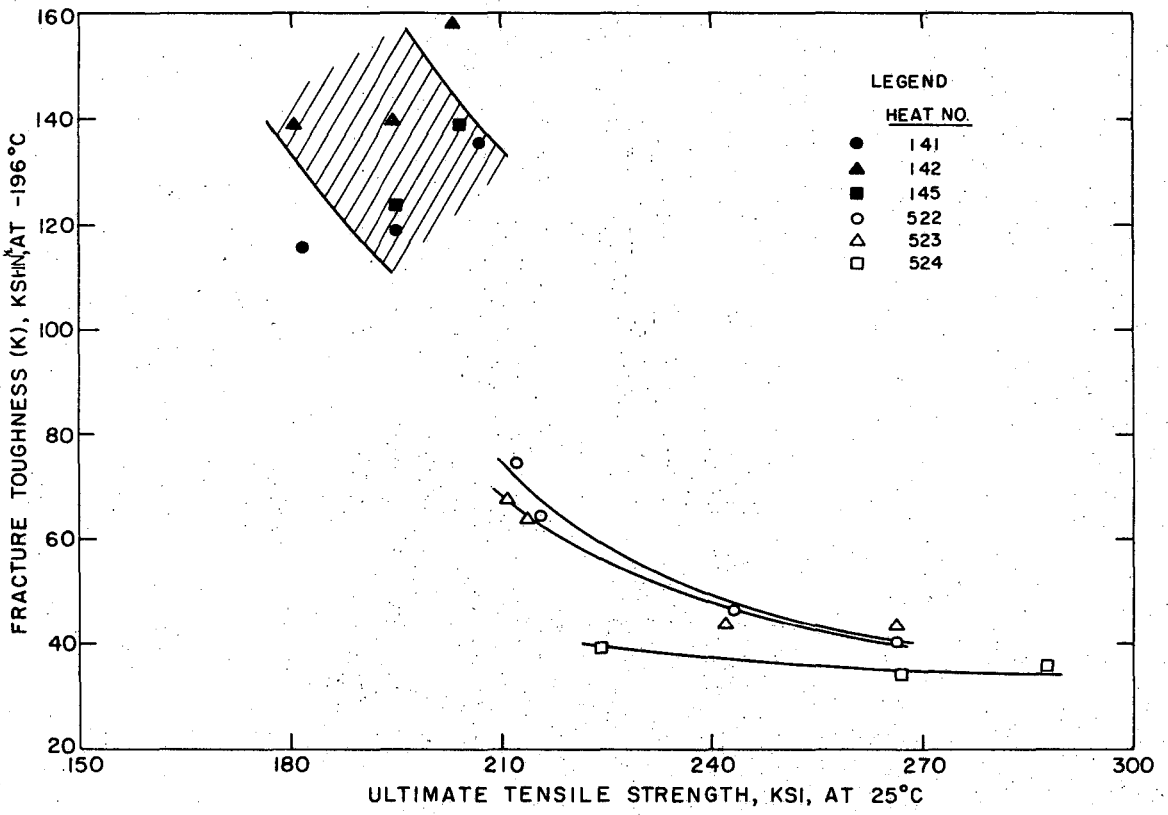

XBL 6811-6180

Figure 9

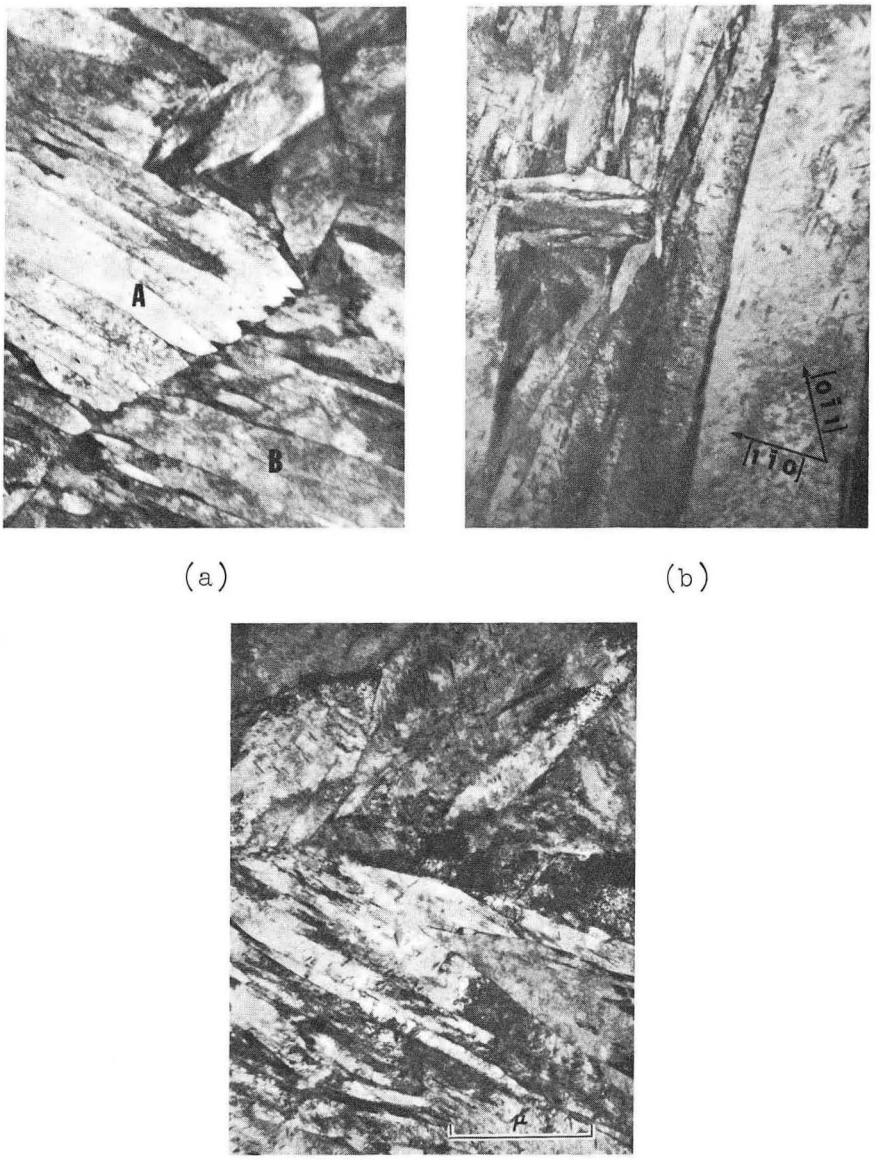

(a) (b)

(c)

XBB 6811-6973

Fig. 10

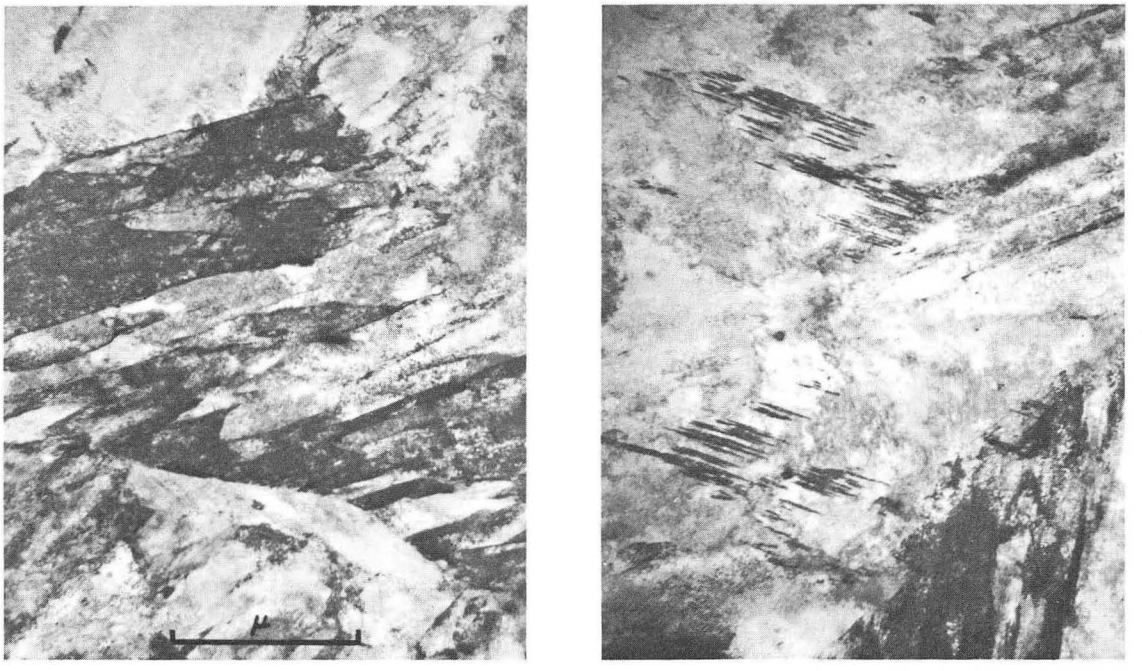

(a) (b) XBB 6811-6964

Fig. 11

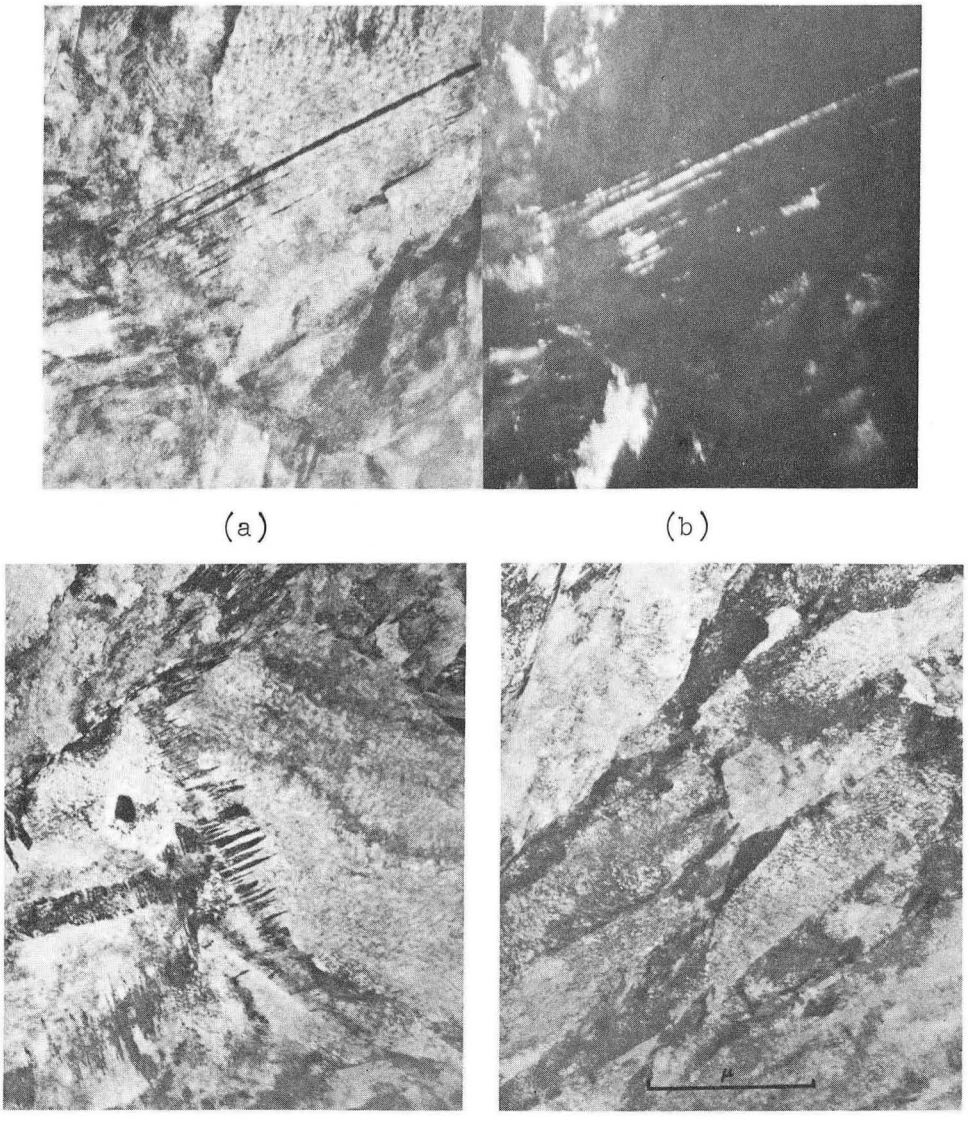

(a) (b)

(c) (d) XBB 6811-6966

Fig. 12

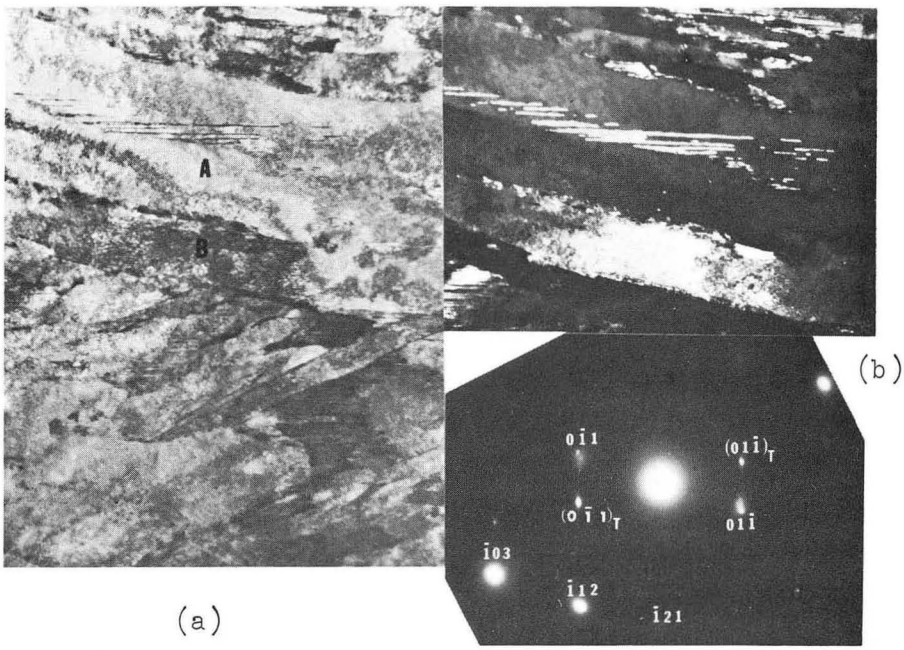

XBB 6811-6962-A

Fig. 13

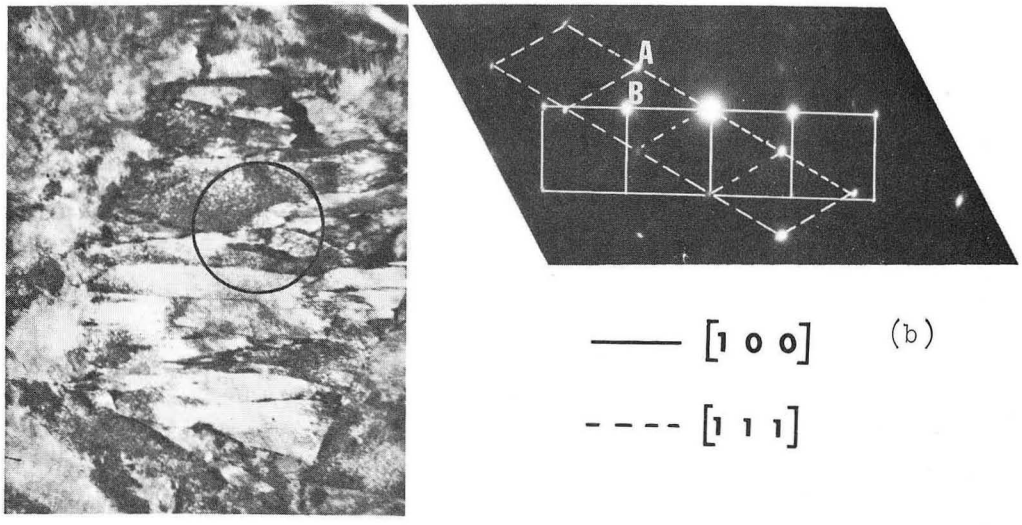

(a)

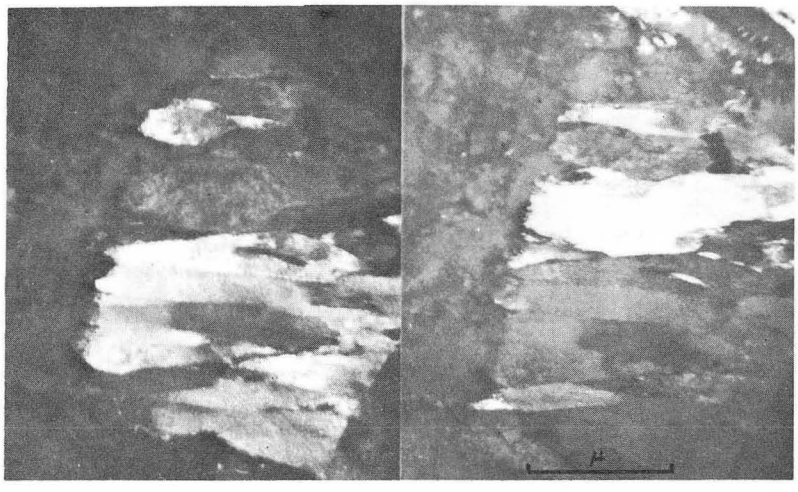

(c) (d)

XBB 6811-6972-A

Fig. 14

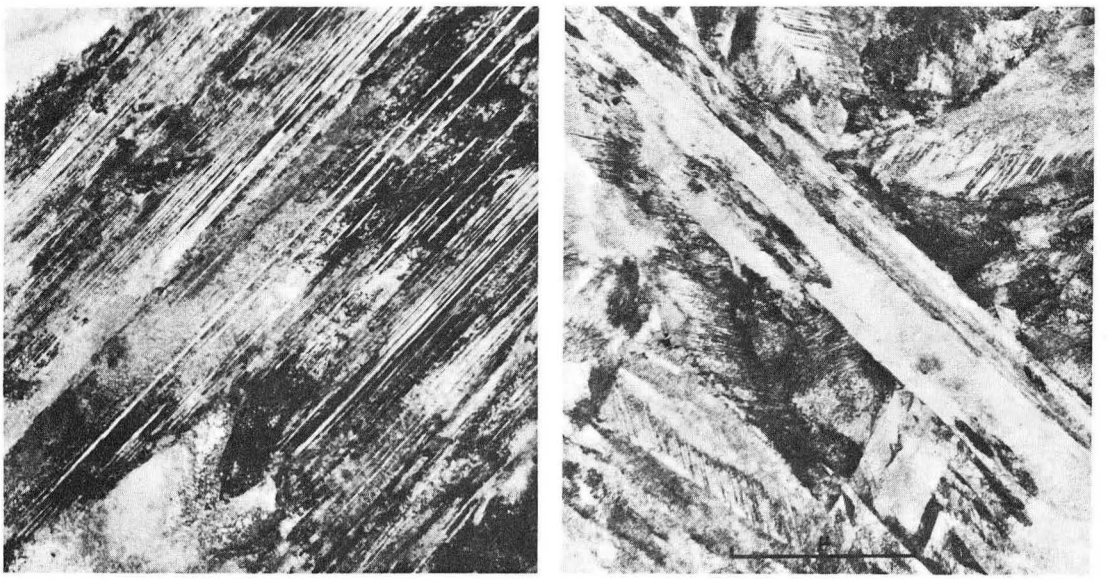

(a) (b) XBB 6811-6970

Fig. 15

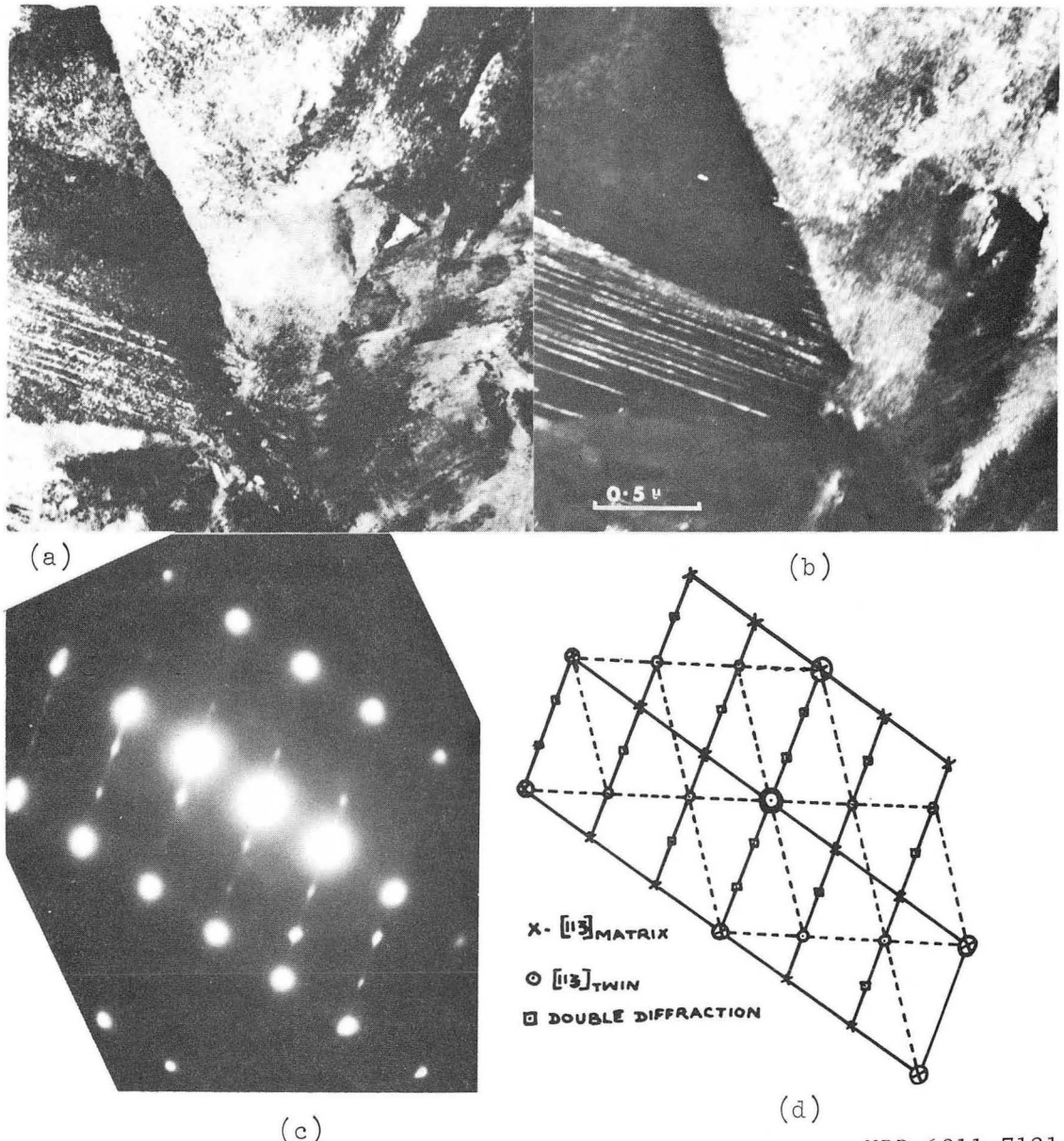

XBB 6811-7121

Fig. 16

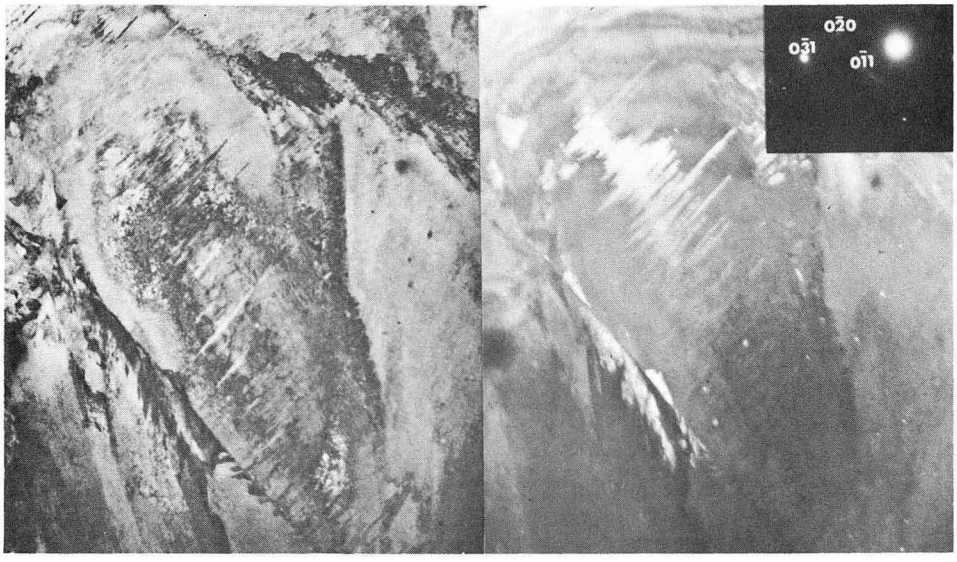

(a) (b)

(c)

XBB 6811-7115

Fig. 17

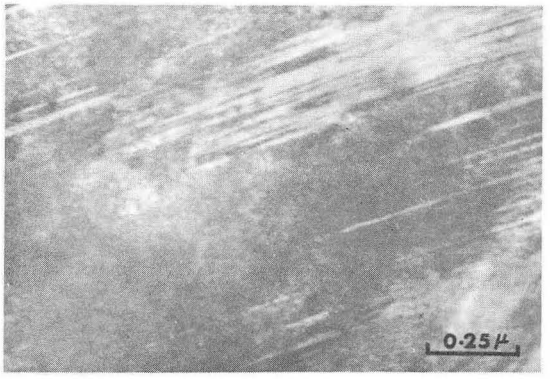

(a)

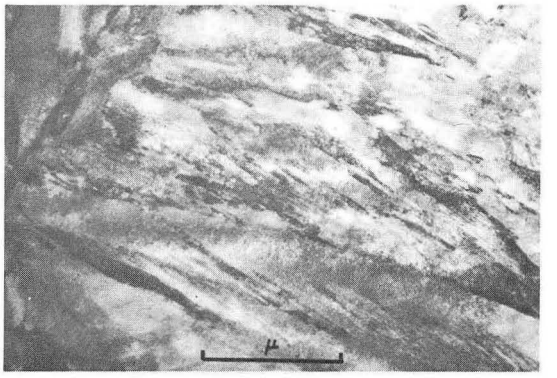

(b)

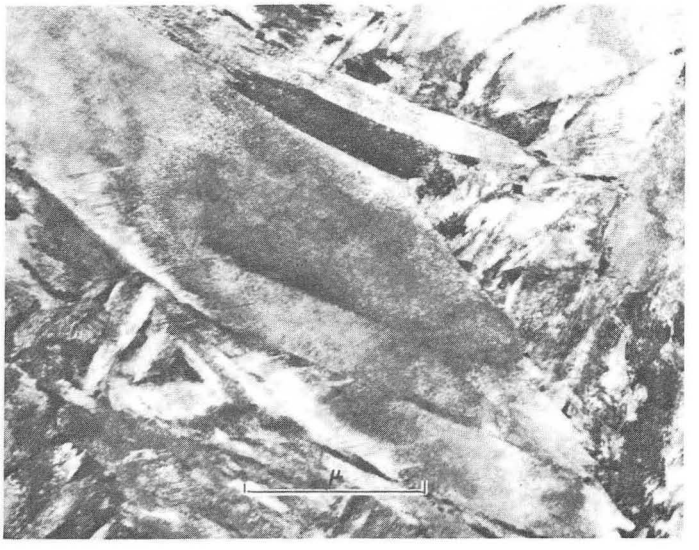

(c)

XBB 6811-6958

Fig. 18

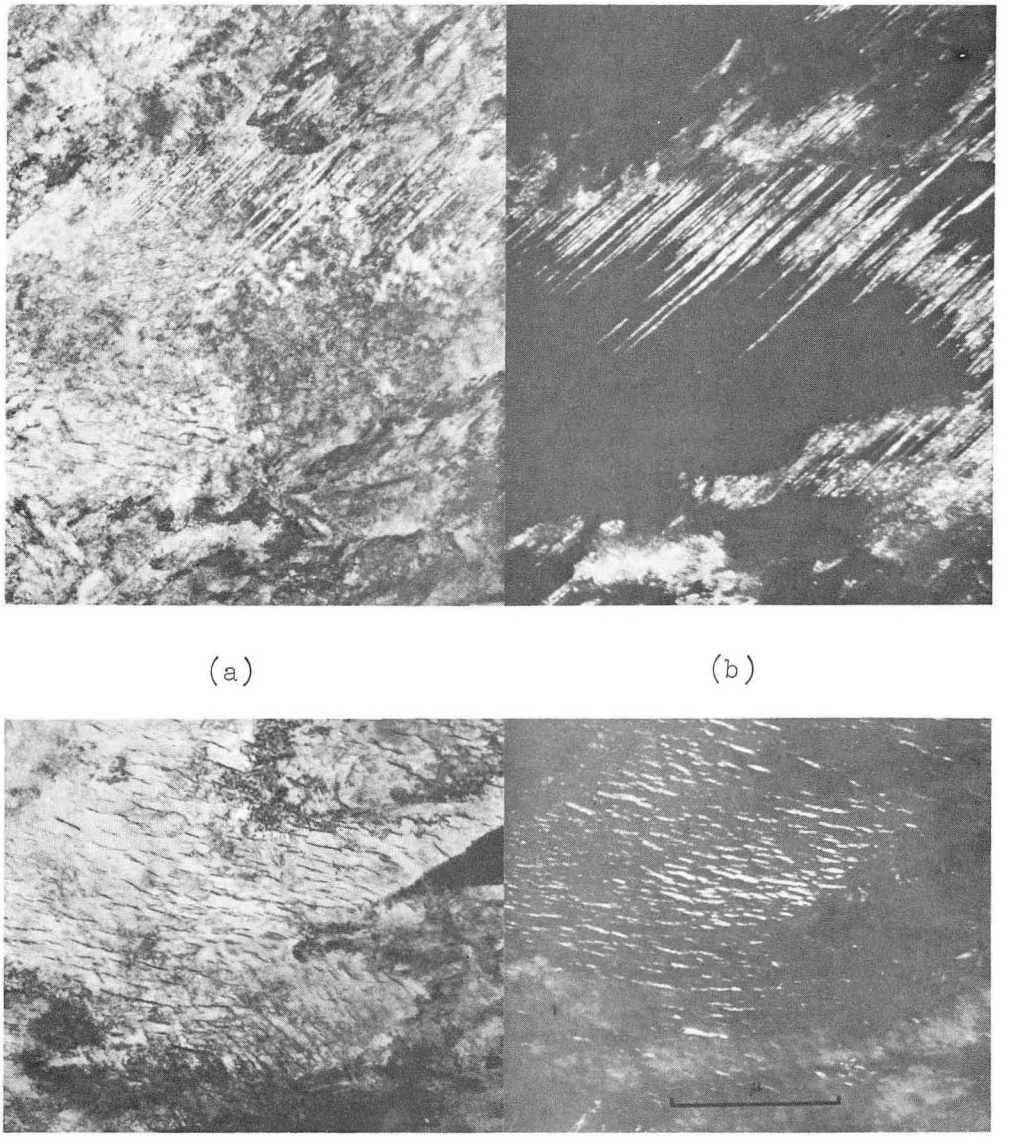

(a) (b)

(c) (d) XBB 6811-6960

Fig. 19

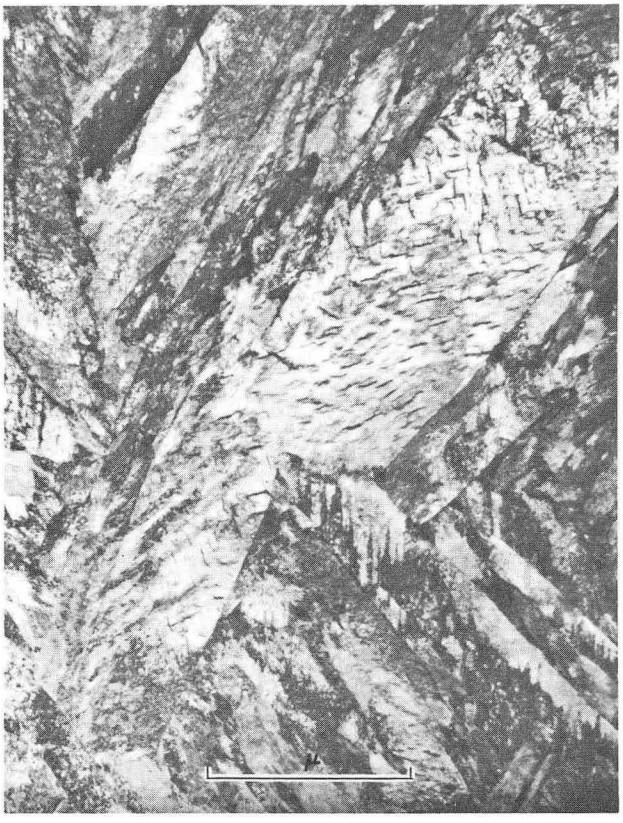

(e)

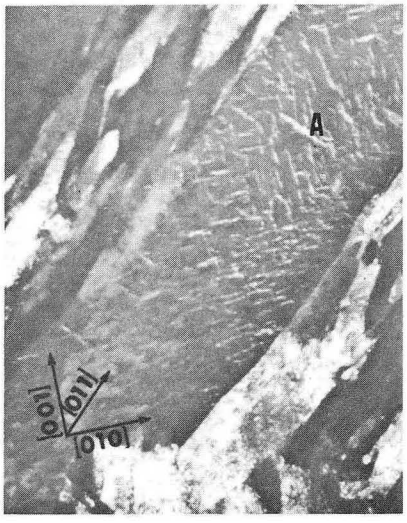

(f)

XBB 6811-6965-A

Fig. 19 (continued)

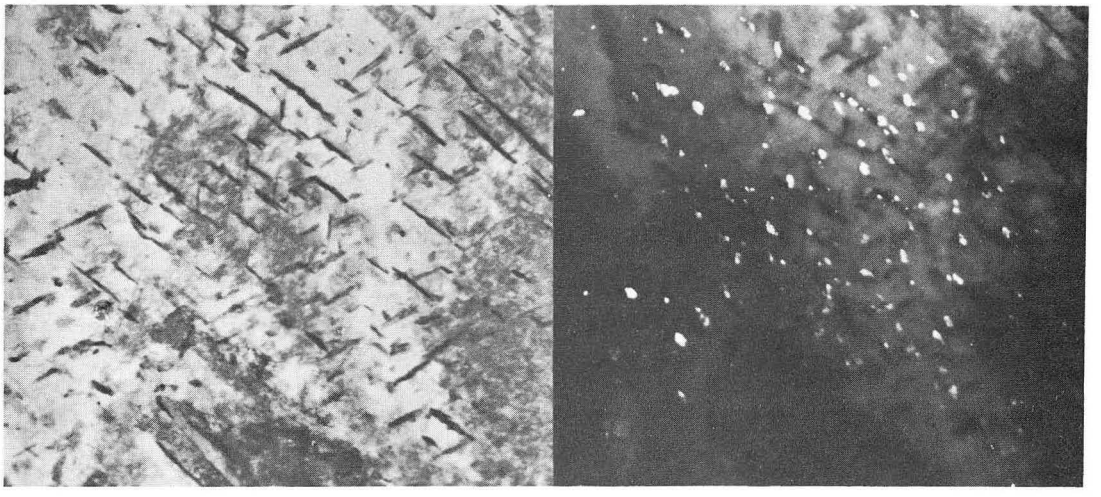

(a) (b)

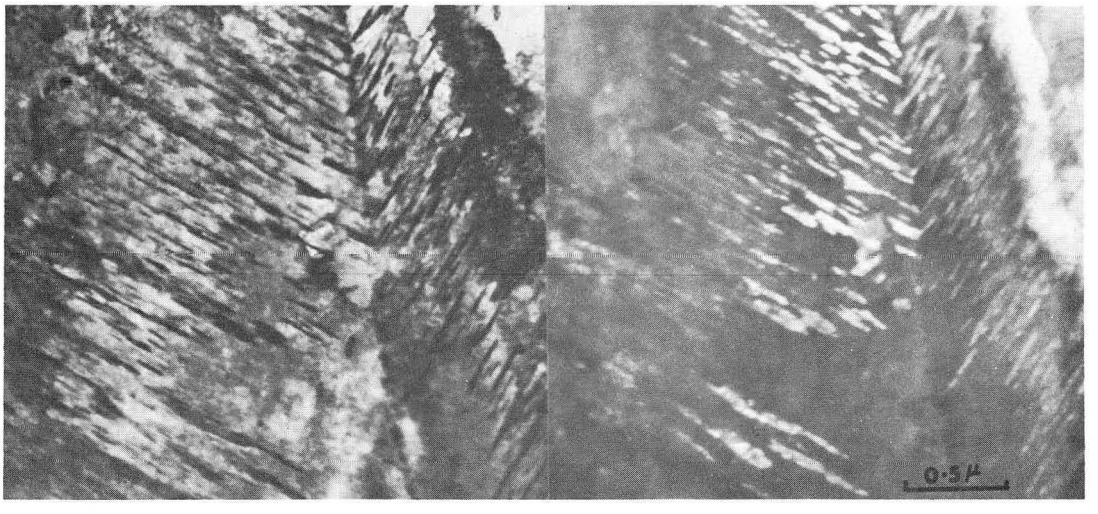

(c) (d) XBB 6811-6968

Fig. 20

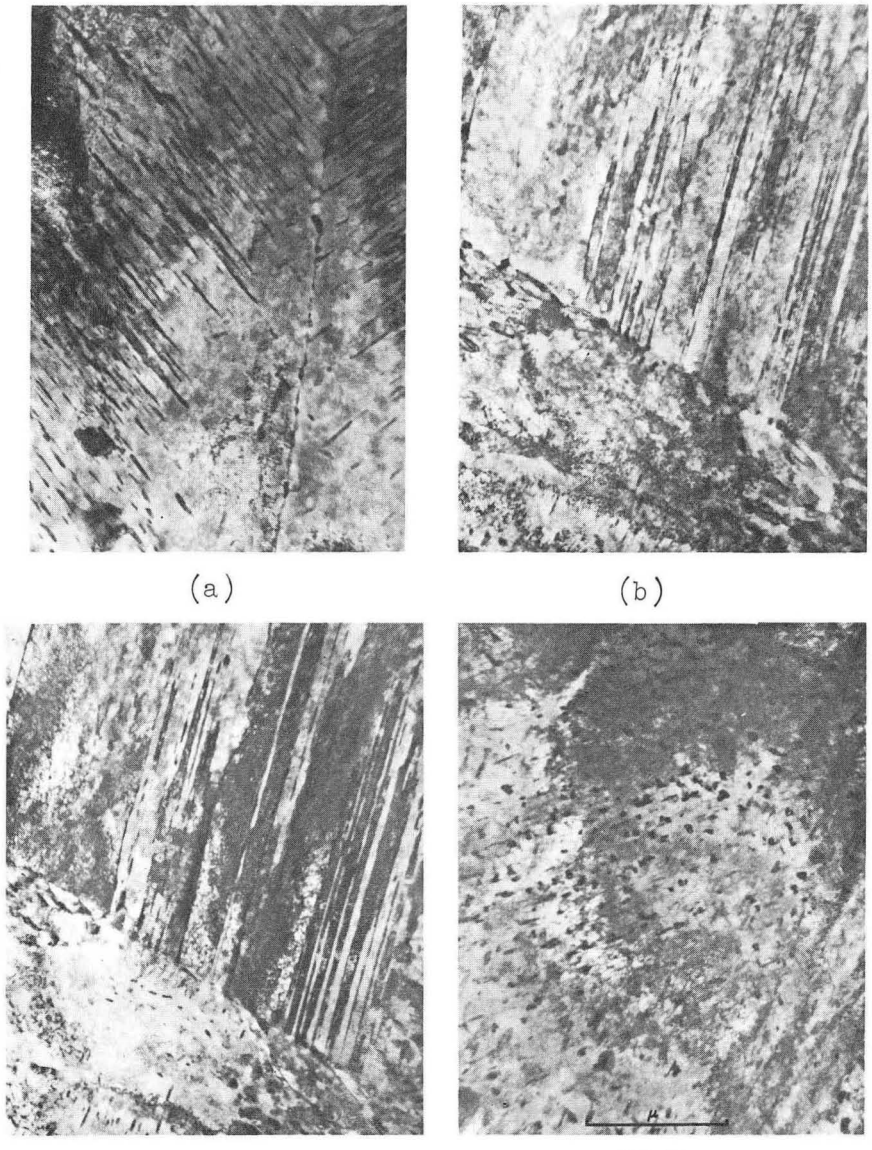

(a) (b)

(c) (d)

XBB 6811-6961

Fig. 21

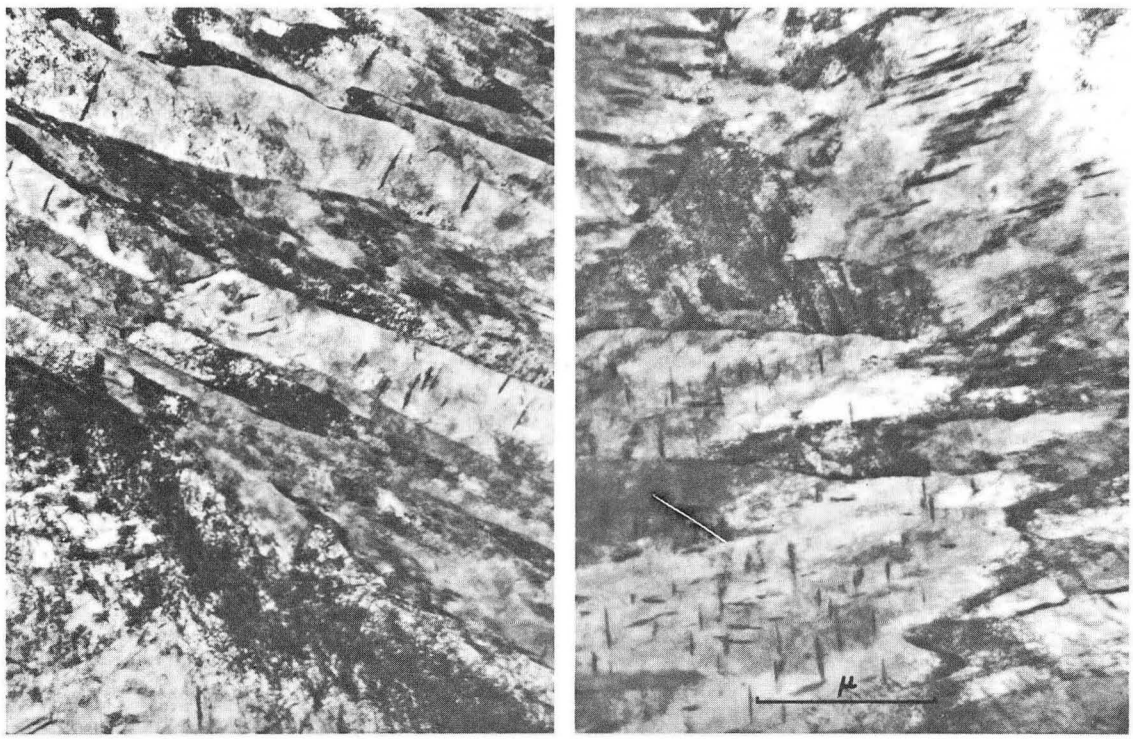

(a) (b) XBB 6811-7119

Fig. 22

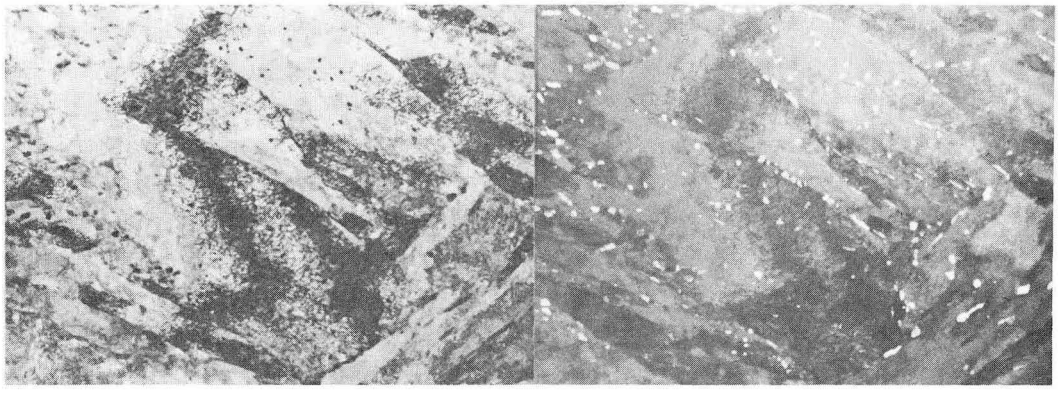

(a) (b)

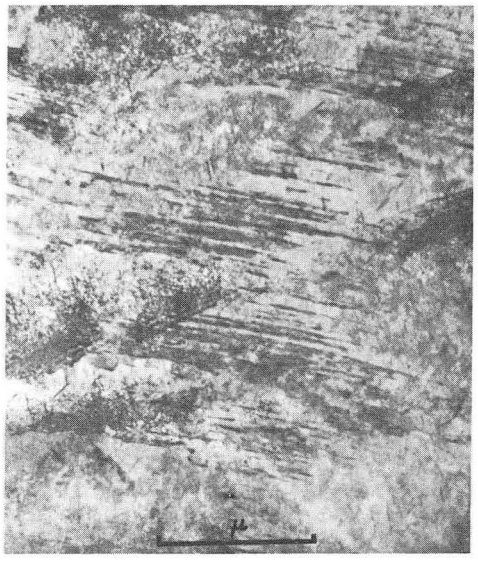

(c)

XBB 6811-6974

Fig. 23

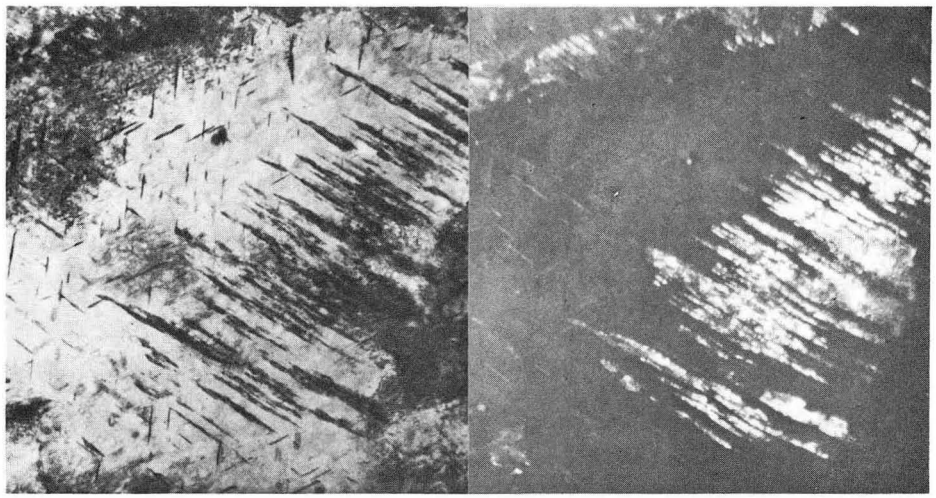

(a) (b)

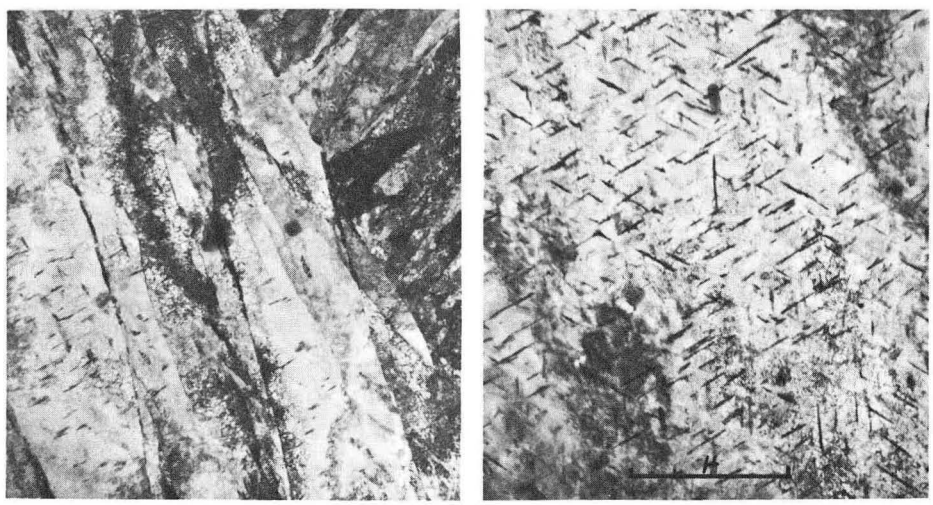

(c) (d) XBB 6811-6967

Fig. 24

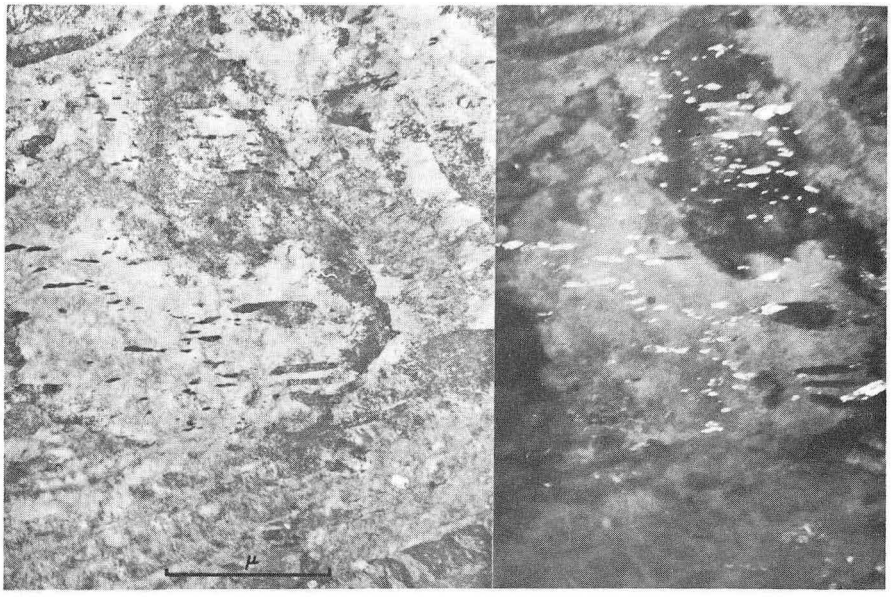

(a) (b)

(c)

XBB 6811-6959

Fig. 25

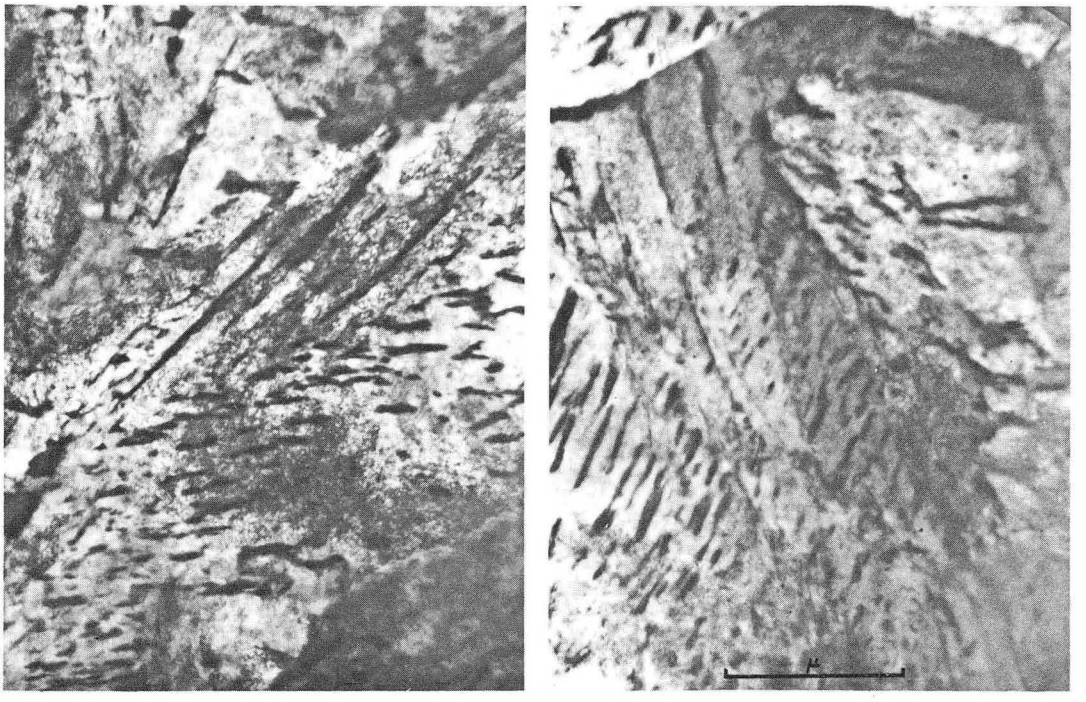

(a) (b) XBB 6811-6969

Fig. 26

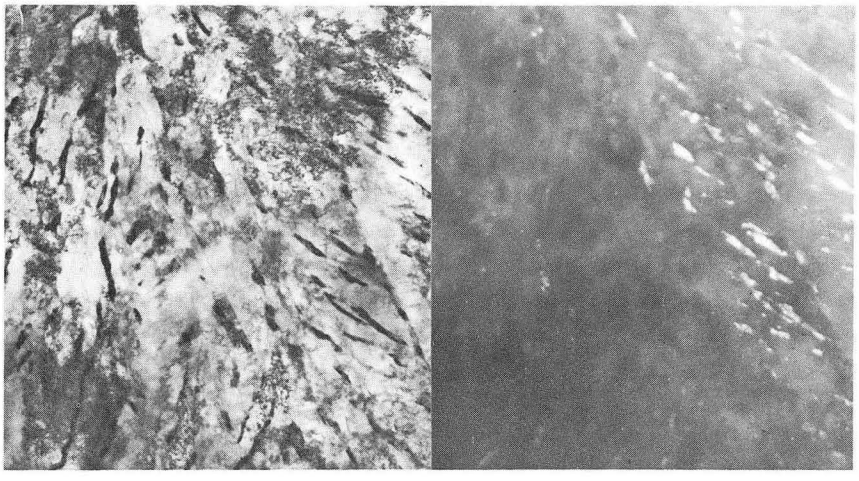

(a) (b)

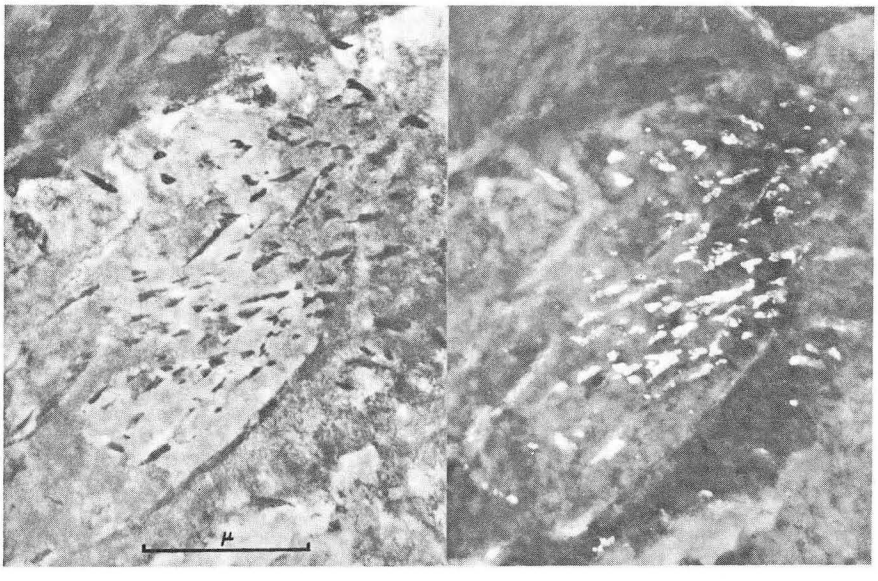

(c) (d) XBB 6811-6963

Fig. 27

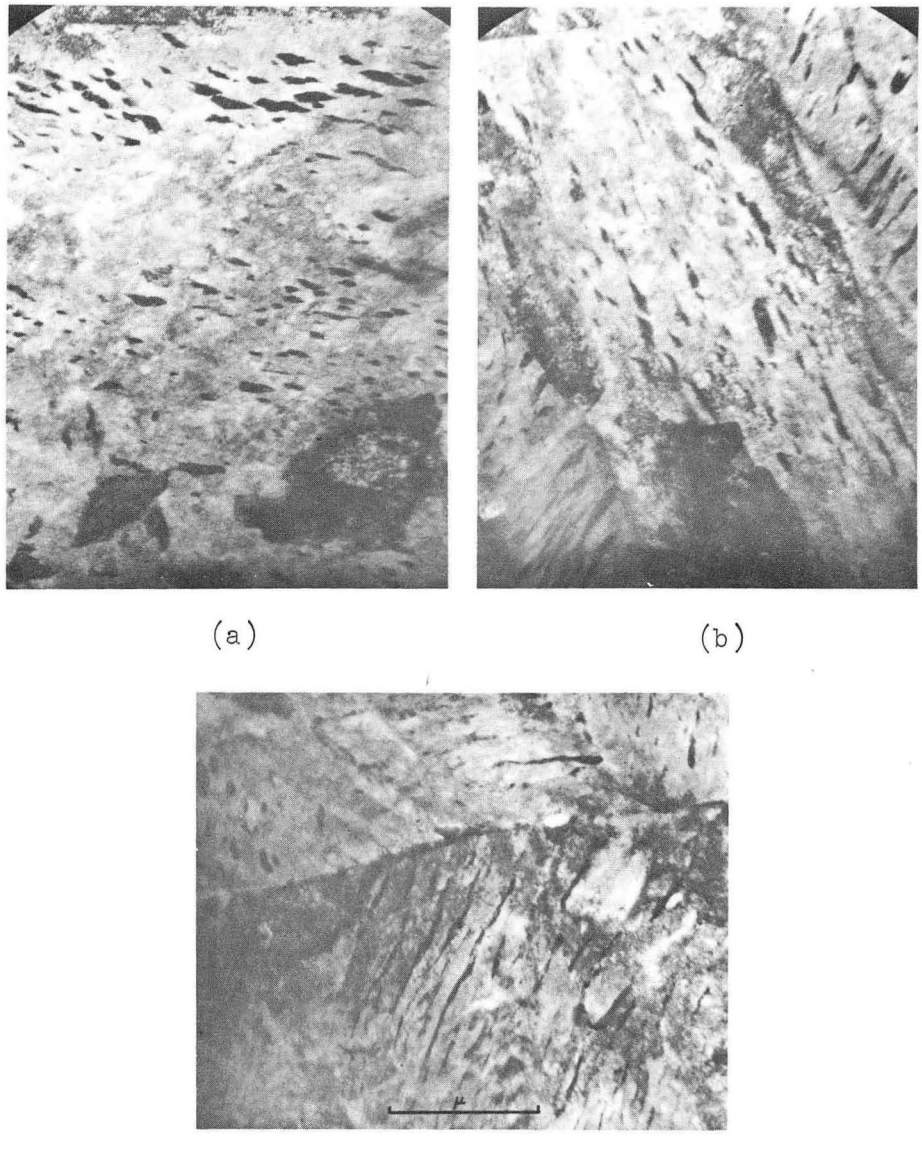

(a) (b)

(c)

XBB 6811-6975

Fig. 28

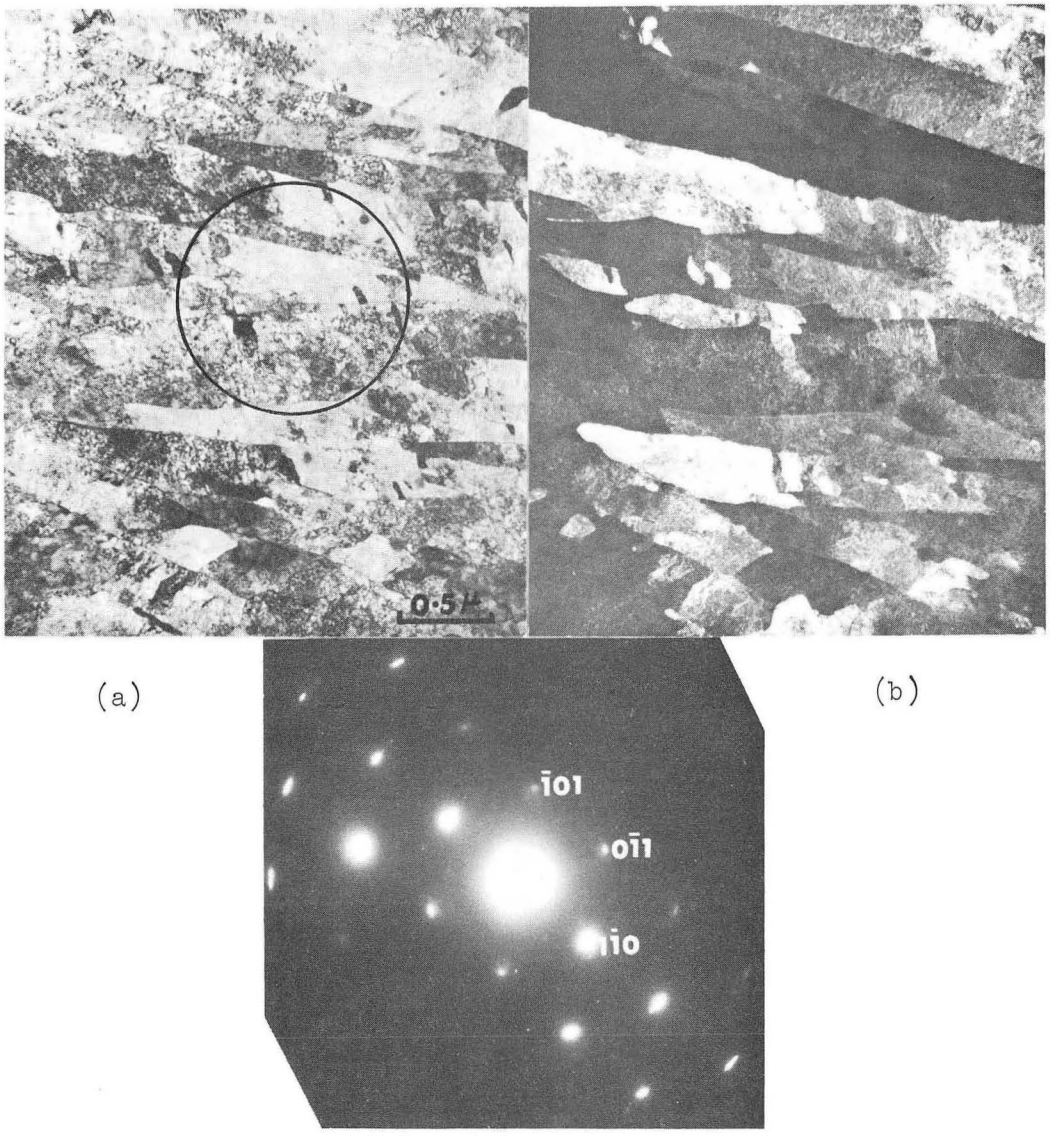

Fig. 29

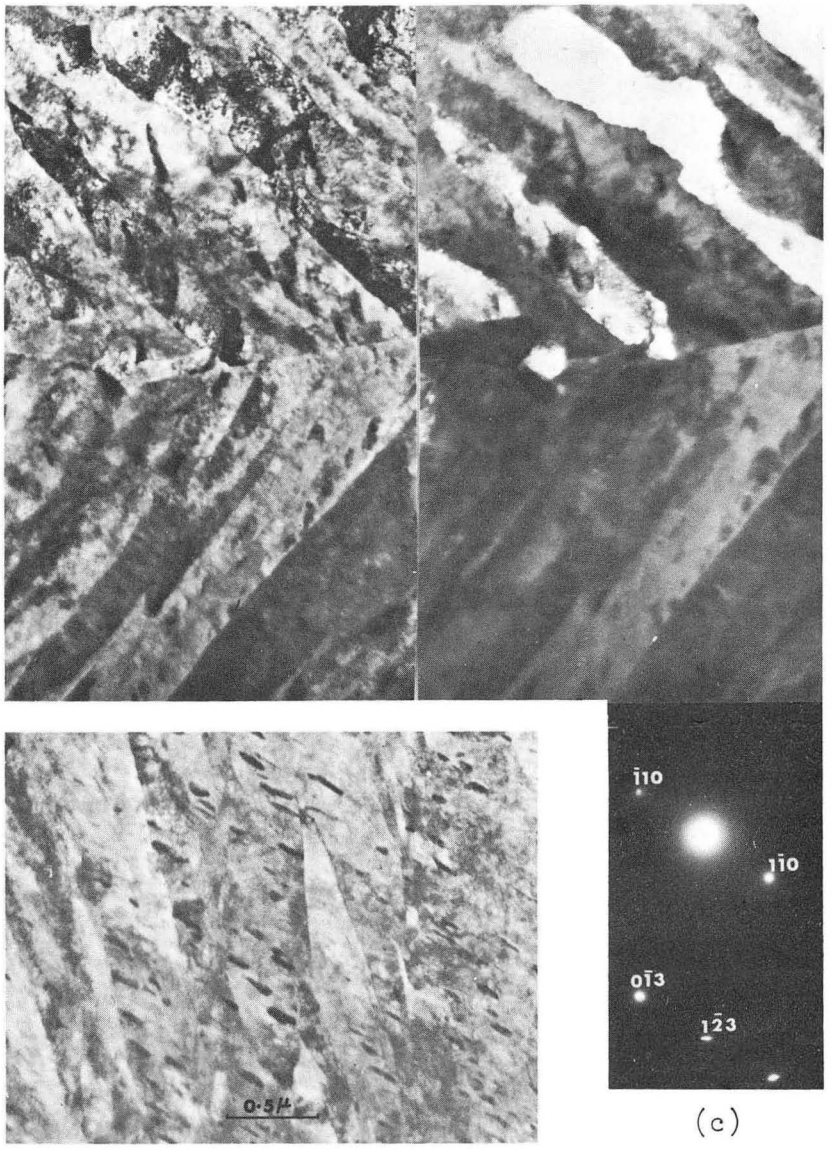

XBB 6811-7118

Fig. 30

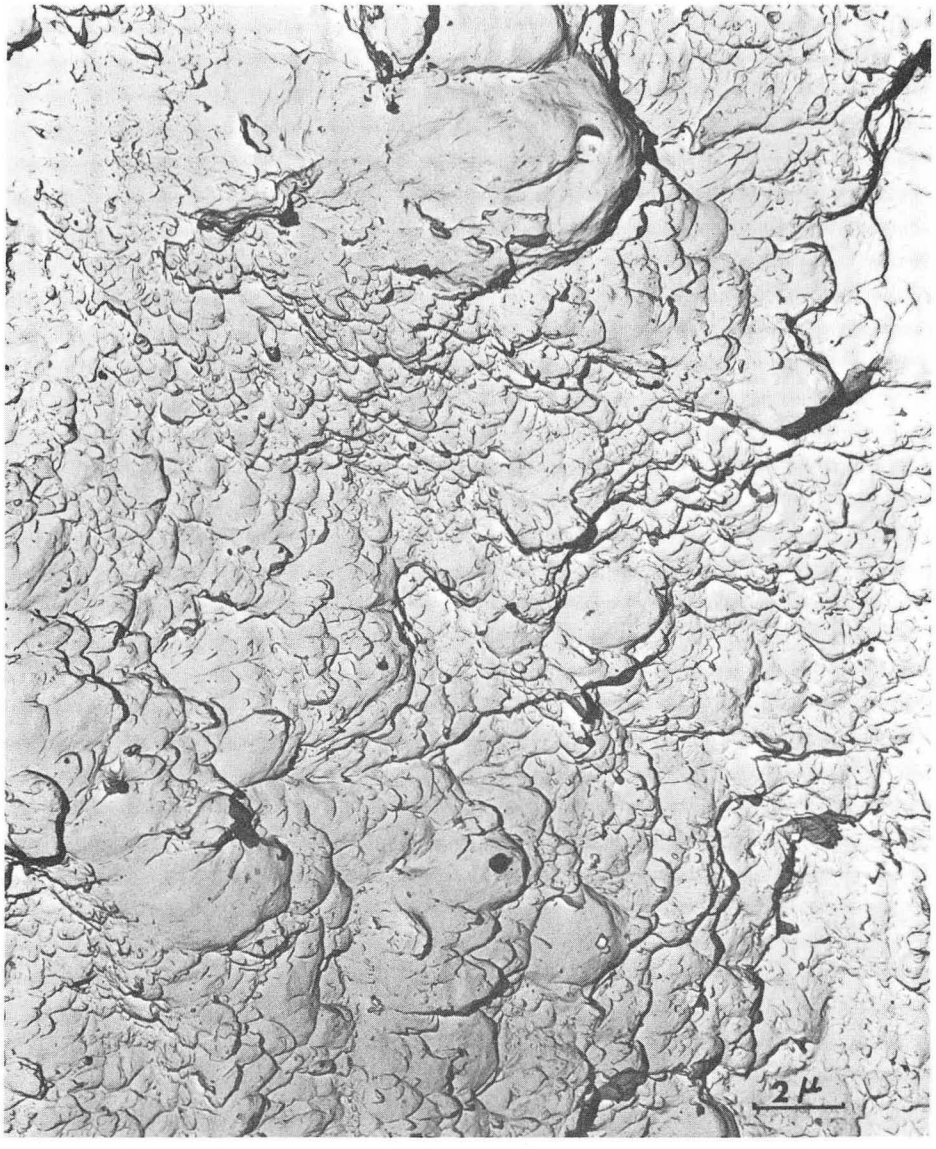

XBB 6811-7120

Fig. 31

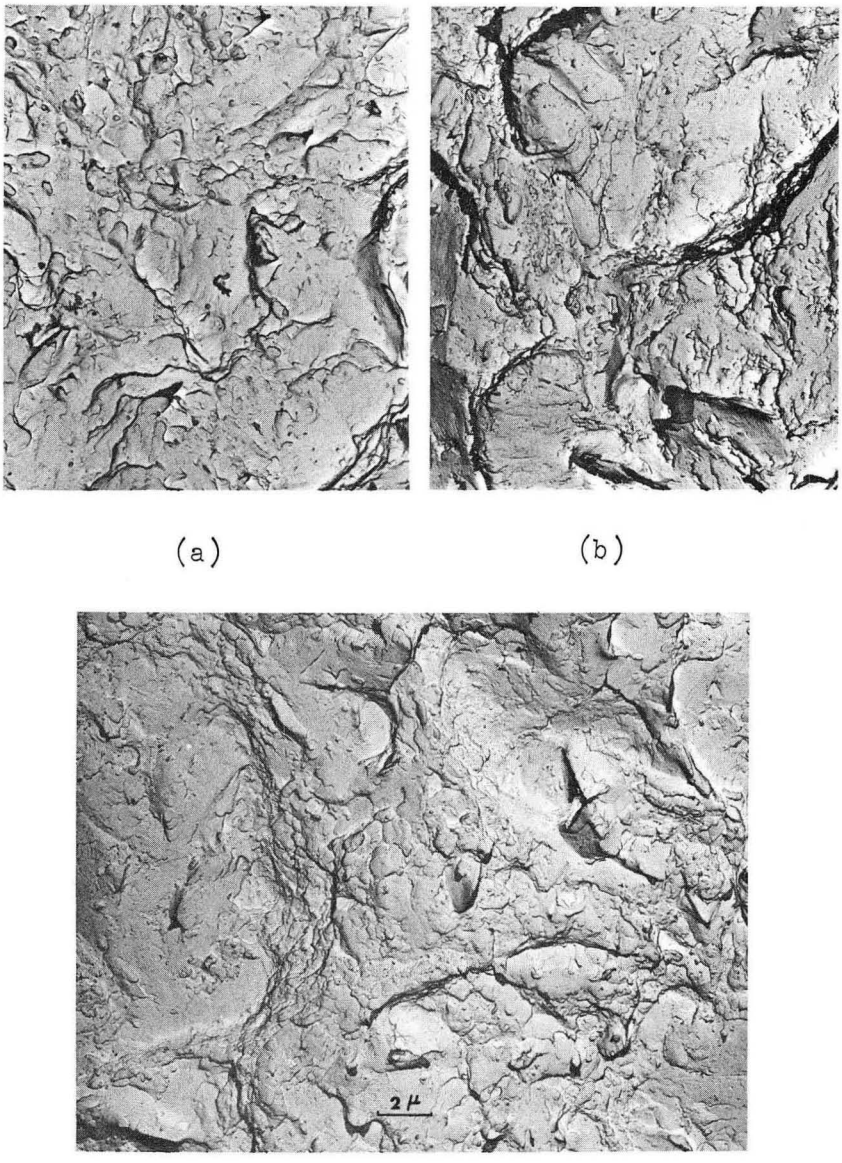

(a) (b)

(c) XBB 6811-7117

Fig. 32

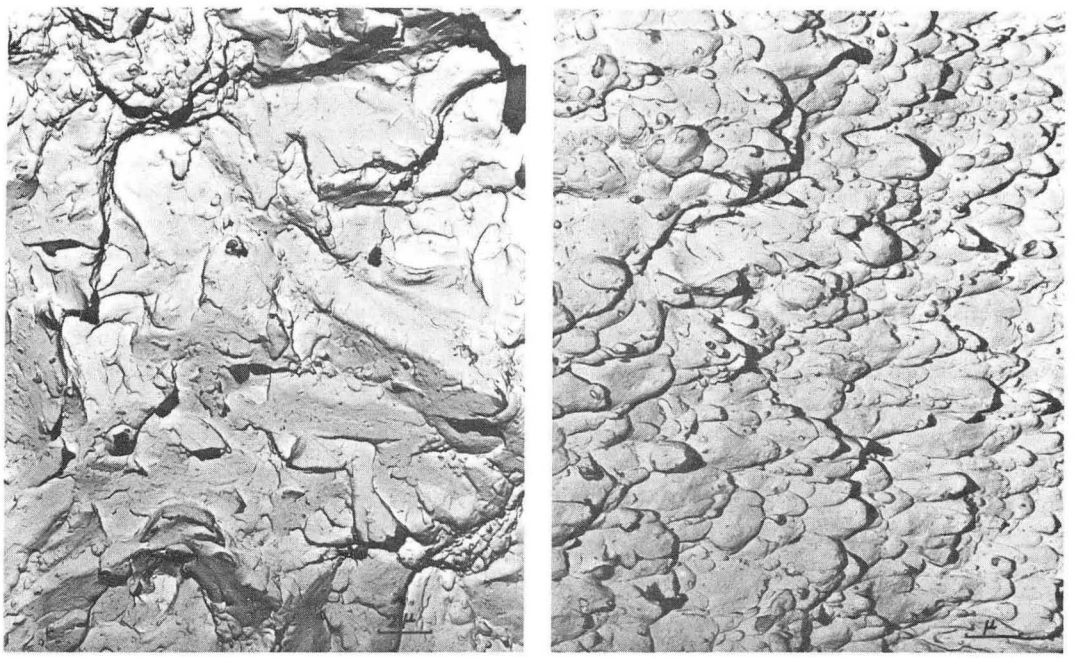

(a) (b)

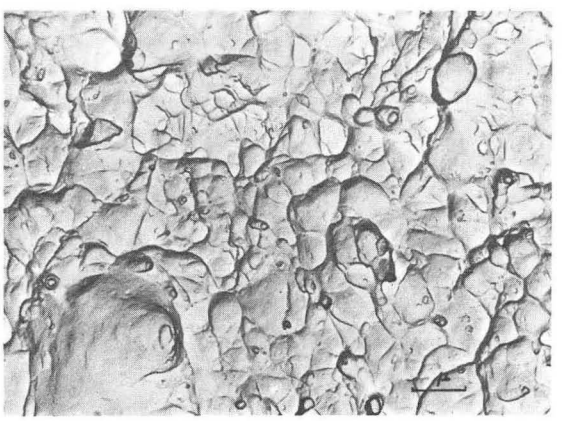

(c) XBB 6811-7114

Fig. 33

LEGAL NOTICE

This report was prepared as an account of Government sponsored work. Neither the United States, nor the Commission, nor any person acting on behalf of the Commission:

A. Makes any warranty or representation, expressed or implied, with respect to the accuracy, completeness, or usefulness of the information contained in this report, or that the use of any information, apparatus, method, or process disclosed in this report may not infringe privately owned rights; or

B. Assumes any liabilities with respect to the use of, or for damages resulting from the use of any information, apparatus, method, or process disclosed in this report.

As used in the above, "person acting on behalf of the Commission" includes any employee or contractor of the Commission, or employee of such contractor, to the extent that such employee or contractor of the Commission, or employee of such contractor prepares, disseminates, or provides access to, any information pursuant to his employment or contract with the Commission, or his employment with such contractor.

TECHNICAL INFORMATION DIVISION
LAWRENCE RADIATION LABORATORY
UNIVERSITY OF CALIFORNIA
BERKELEY, CALIFORNIA 94720